SUPPORTING INFORMATION

Synthesis and studies on forward and reverse reactions of phenol-blocked polyisocyanates: An insight into blocked isocyanates

A. Sultan Nasar* and S. Kalaimani

Department of Polymer Science, University of Madras, Guindy Campus, Chennai-600025, India.

E-mail: drasultannasar@yahoo.com; drasultannasar@unom.ac.in; Tel: +044-22202820

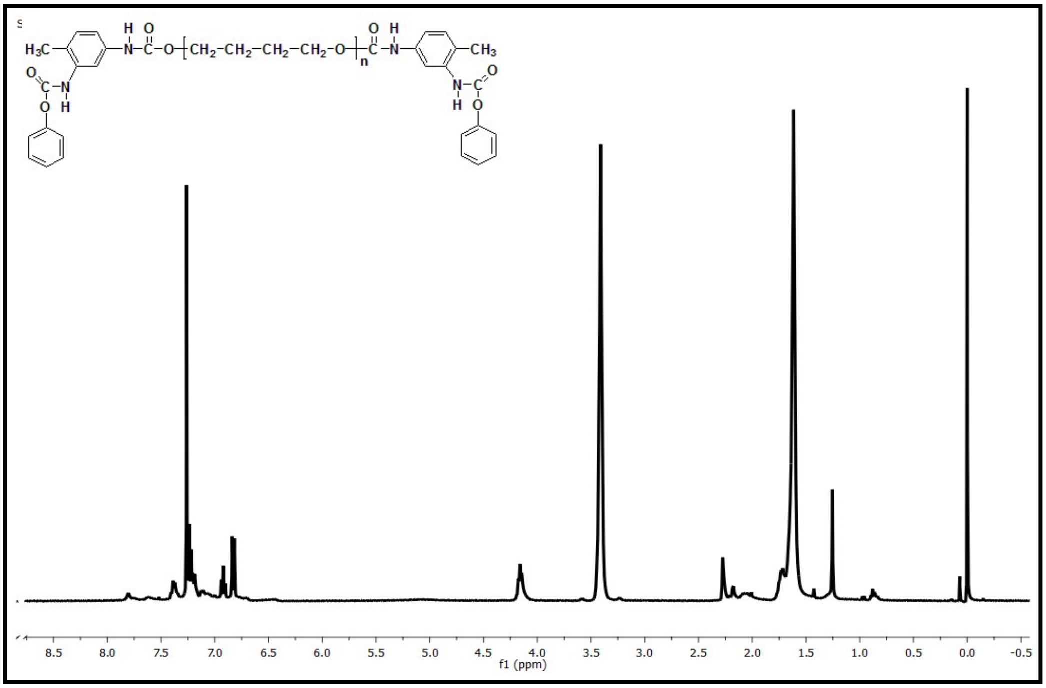

Figure S1. ^{1}H-NMR spectrum of phenol-blocked polyisocyanate (Solvent:$CDCl_3$).

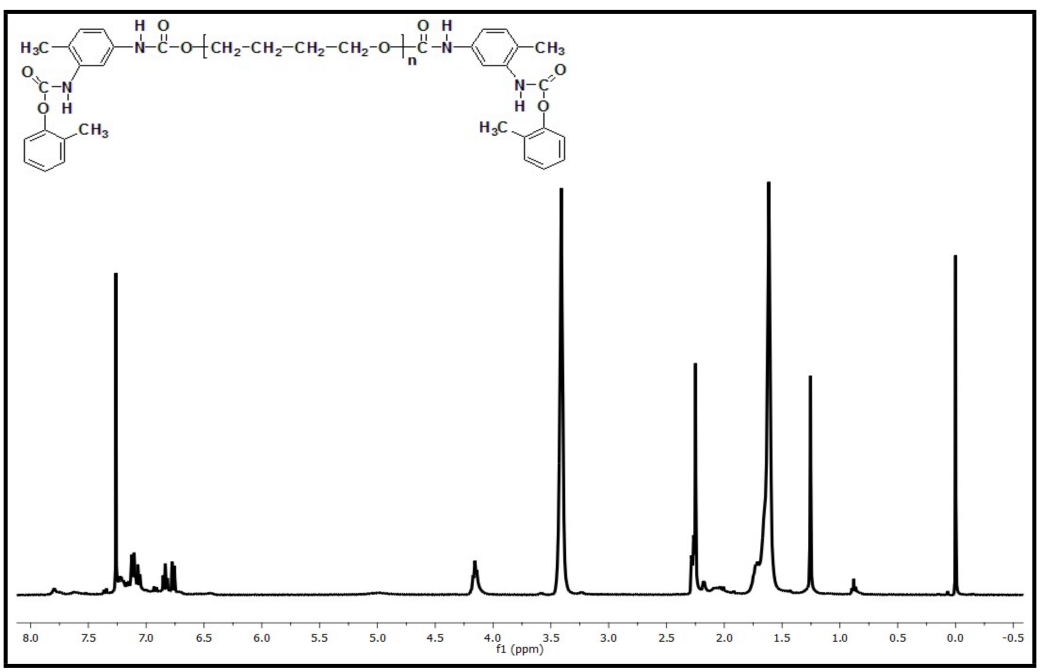

Figure S2. ^{1}H-NMR spectrum of o-cresol-blocked polyisocyanate (Solvent:$CDCl_3$).

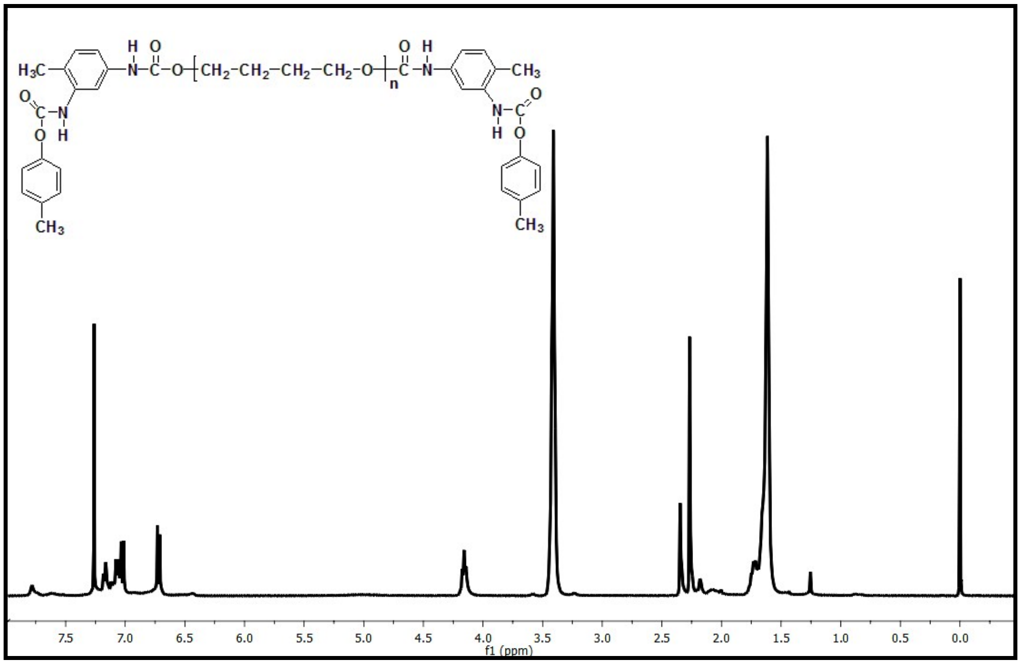

Figure S3. ^{1}H-NMR spectrum of p-cresol-blocked polyisocyanate (Solvent:$CDCl_3$).

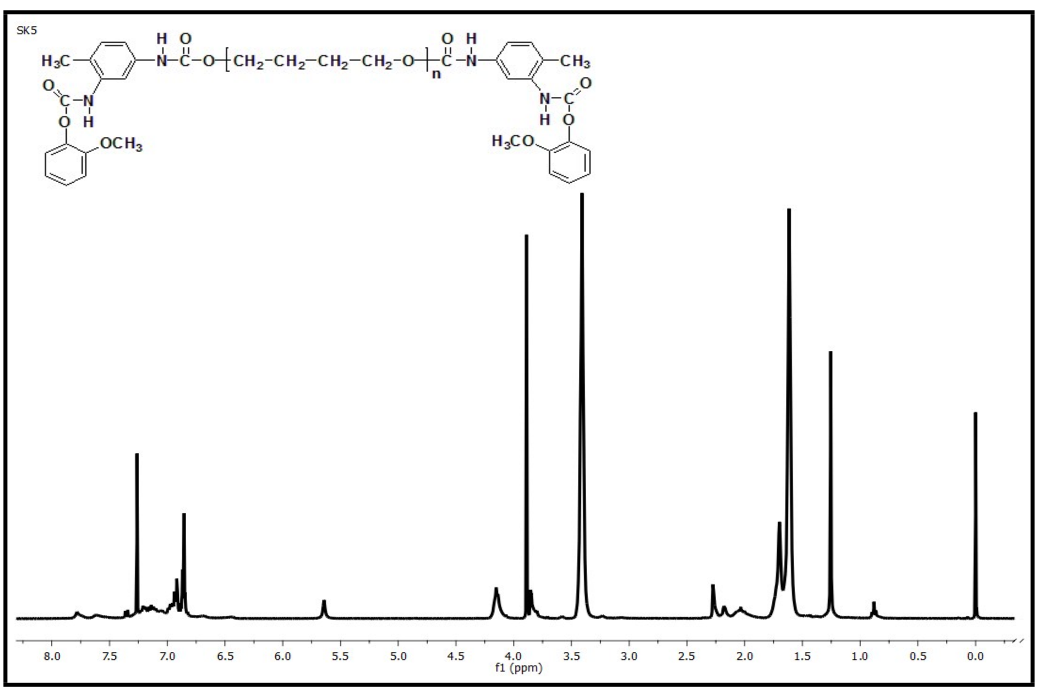

Figure S4. ^{1}H-NMR spectrum of o-methoxyphenol-blocked polyisocyanate (Solvent:$CDCl_3$).

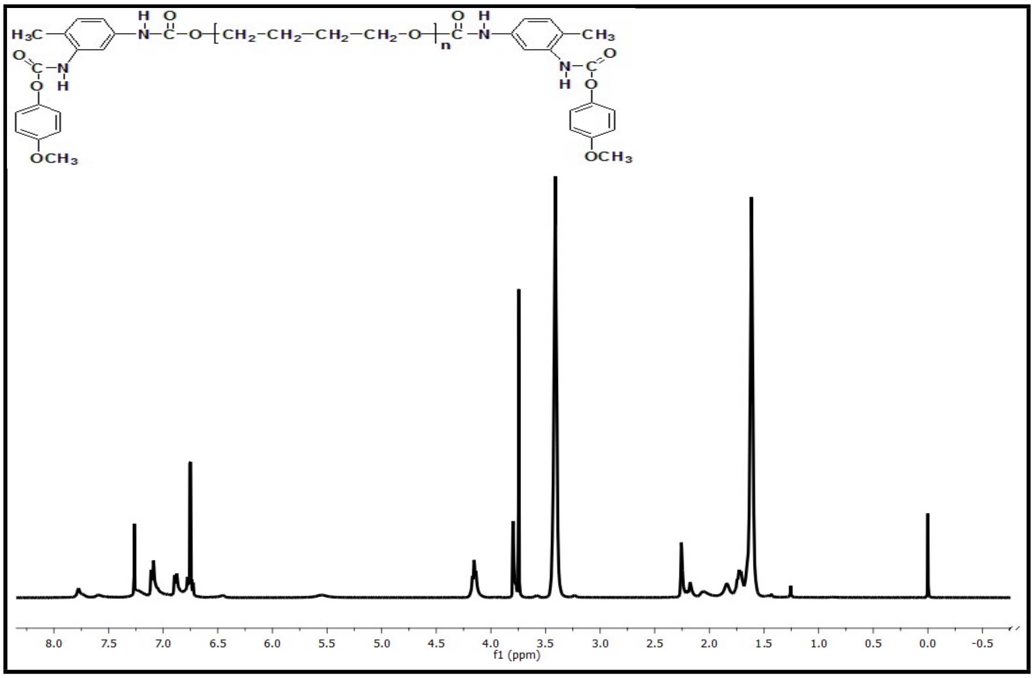

Figure S5. [1]H-NMR spectrum of p-methoxyphenol-blocked polyisocyanate (Solvent:$CDCl_3$)**.**

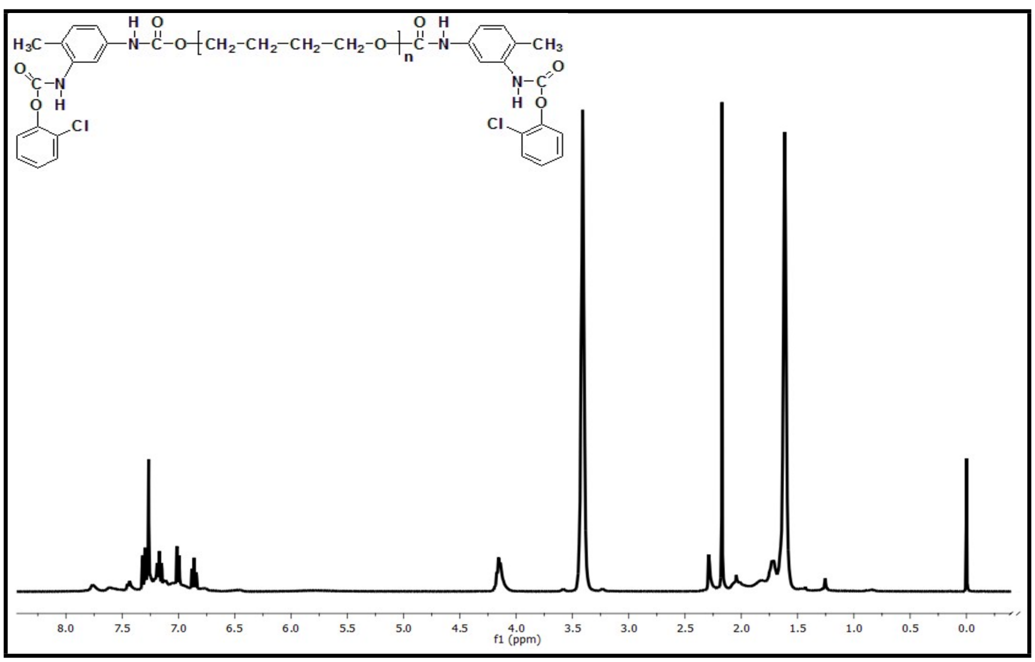

Figure S6. [1]H-NMR spectrum of o-chlorophenol-blocked polyisocyanate (Solvent:$CDCl_3$)**.**

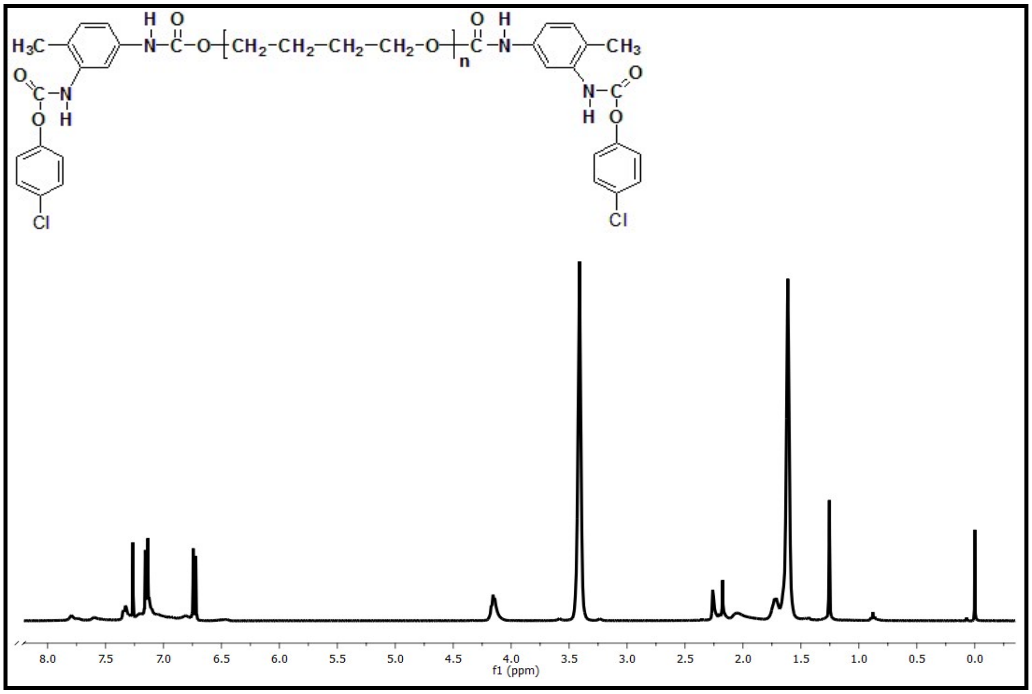

Figure S7. ^{1}H-NMR spectrum of p-chlorophenol-blocked polyisocyanate (Solvent:$CDCl_3$).

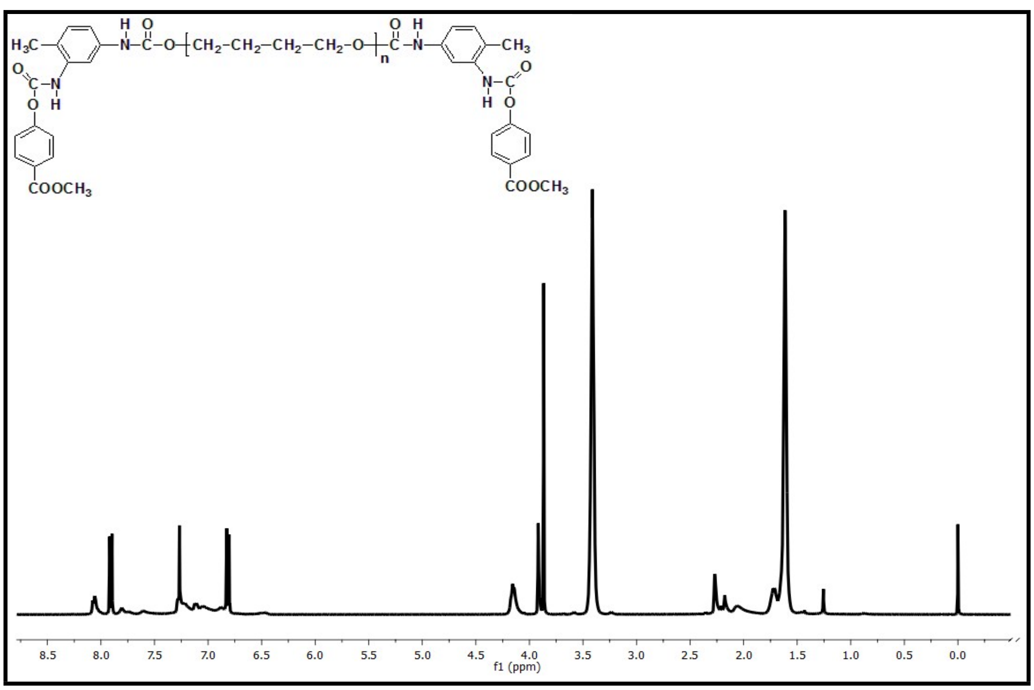

Figure S8. ^{1}H-NMR spectrum of p-esterphenol-blocked polyisocyanate (Solvent:$CDCl_3$).

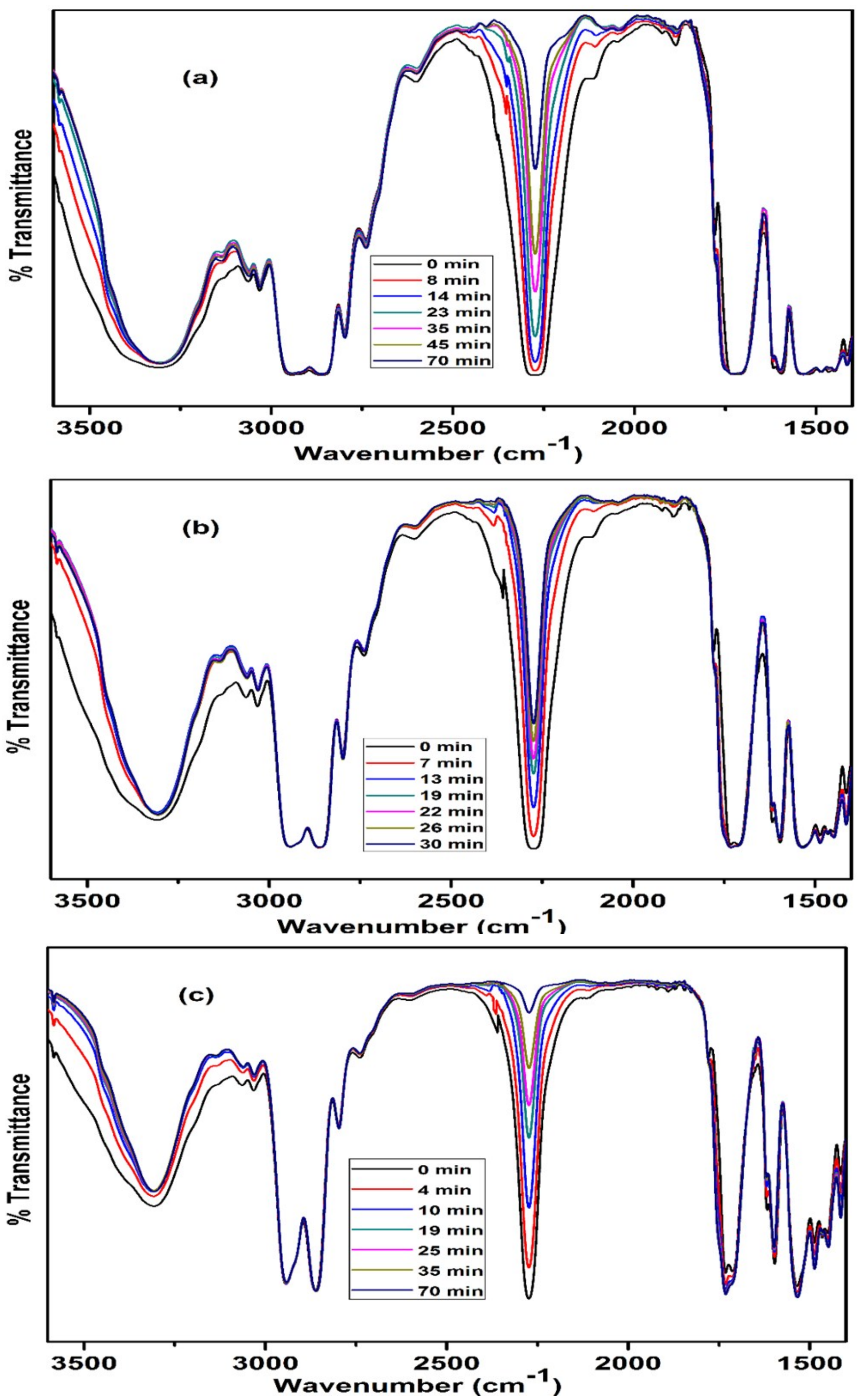

Figure S9. FT-IR Spectra recorded for different time intervals at different temperatures for the blocking reaction of polyisocyanate with o-cresol; (a) 40 ^{0}C (b) 50 ^{0}C and (c) 60 ^{0}C.

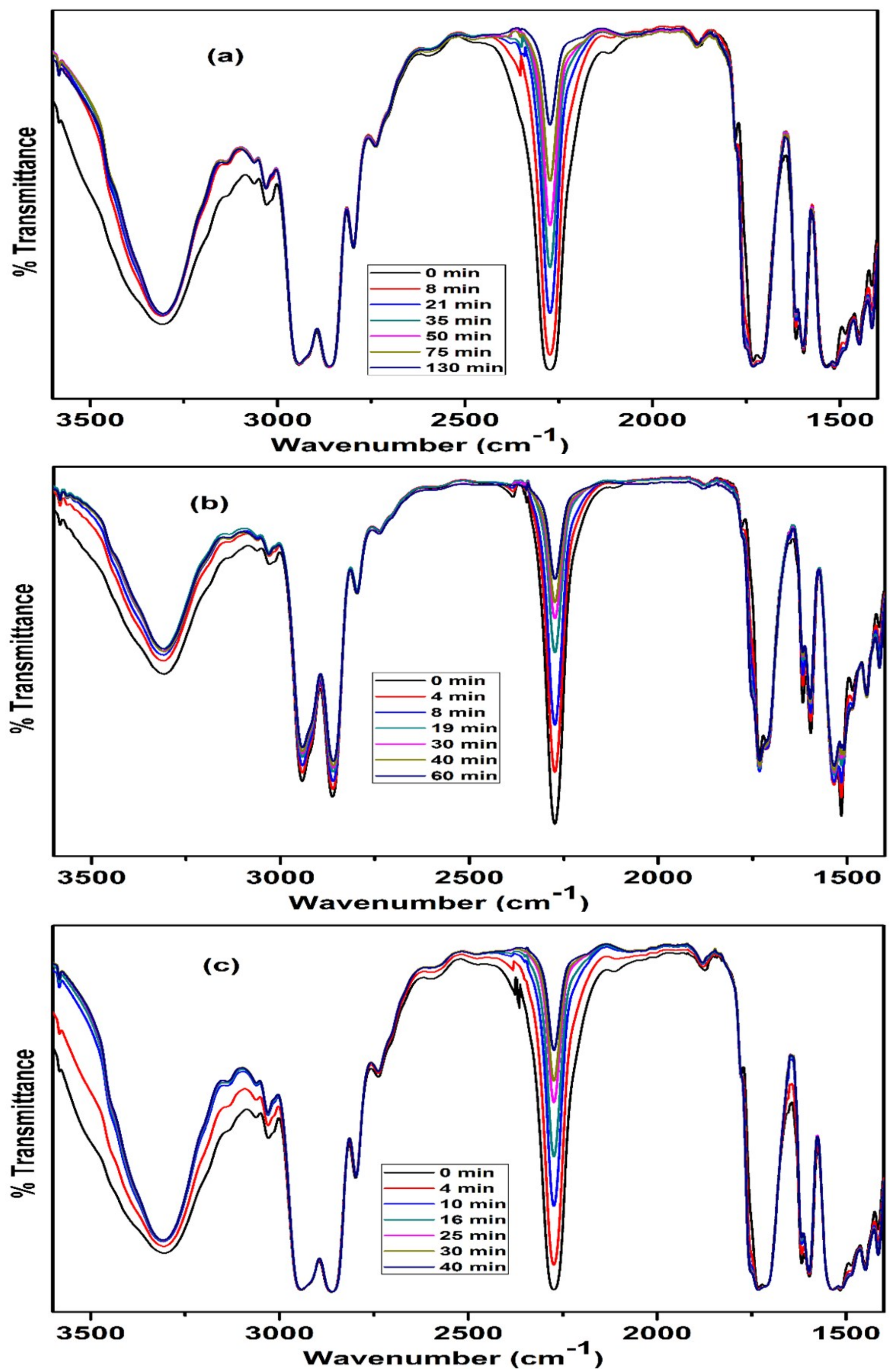

Figure S10. FT-IR Spectra recorded for different time intervals at different temperatures for the blocking reaction of polyisocyanate with p-cresol; (a) 40 ^{0}C (b) 50 ^{0}C and (c) 60 ^{0}C.

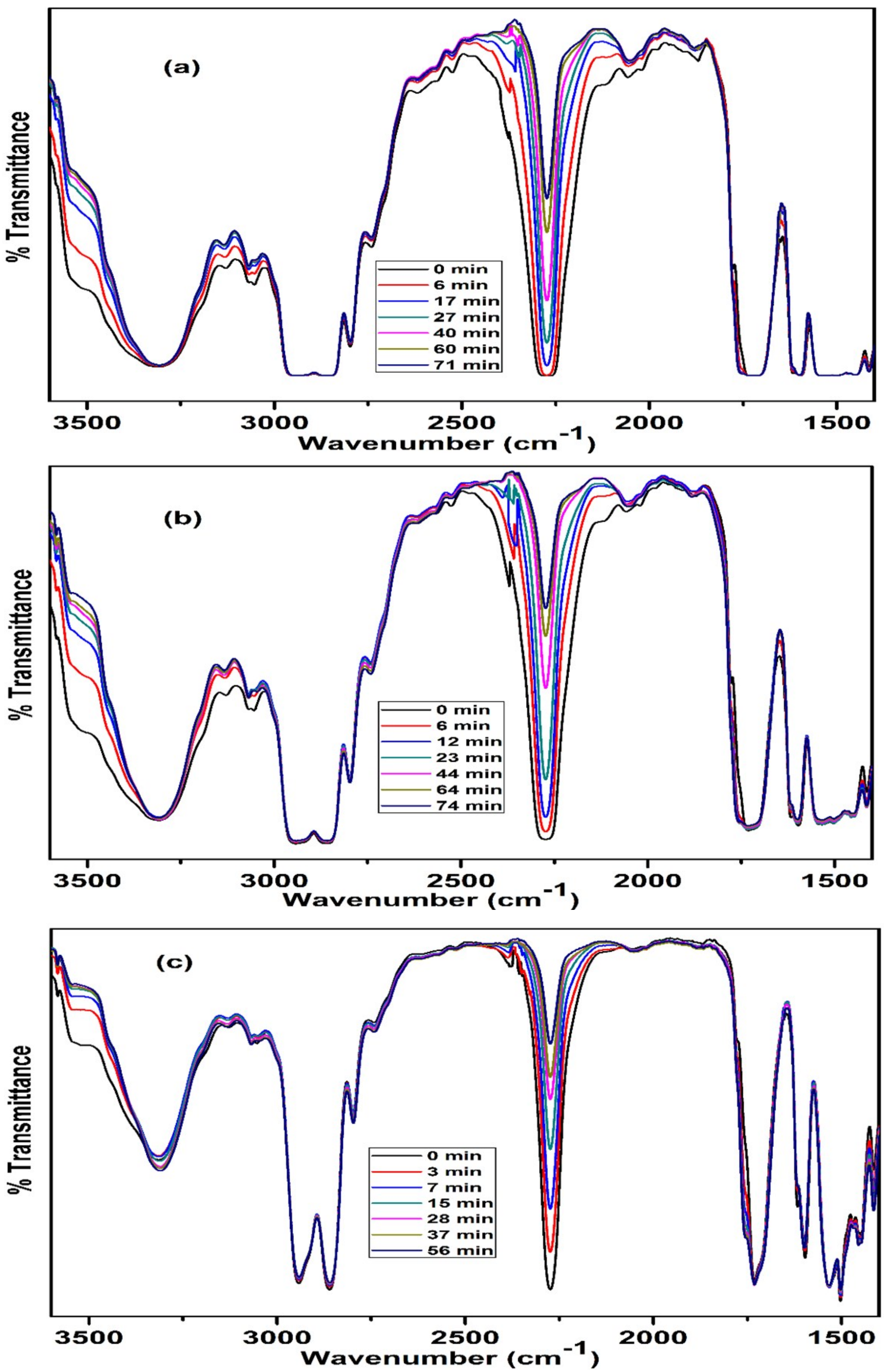

Figure S11. FT-IR Spectra recorded for different time intervals at different temperatures for the blocking reaction of polyisocyanate with o-methoxyphenol; (a) 40 ^{0}C (b) 50 ^{0}C and (c) 60 ^{0}C.

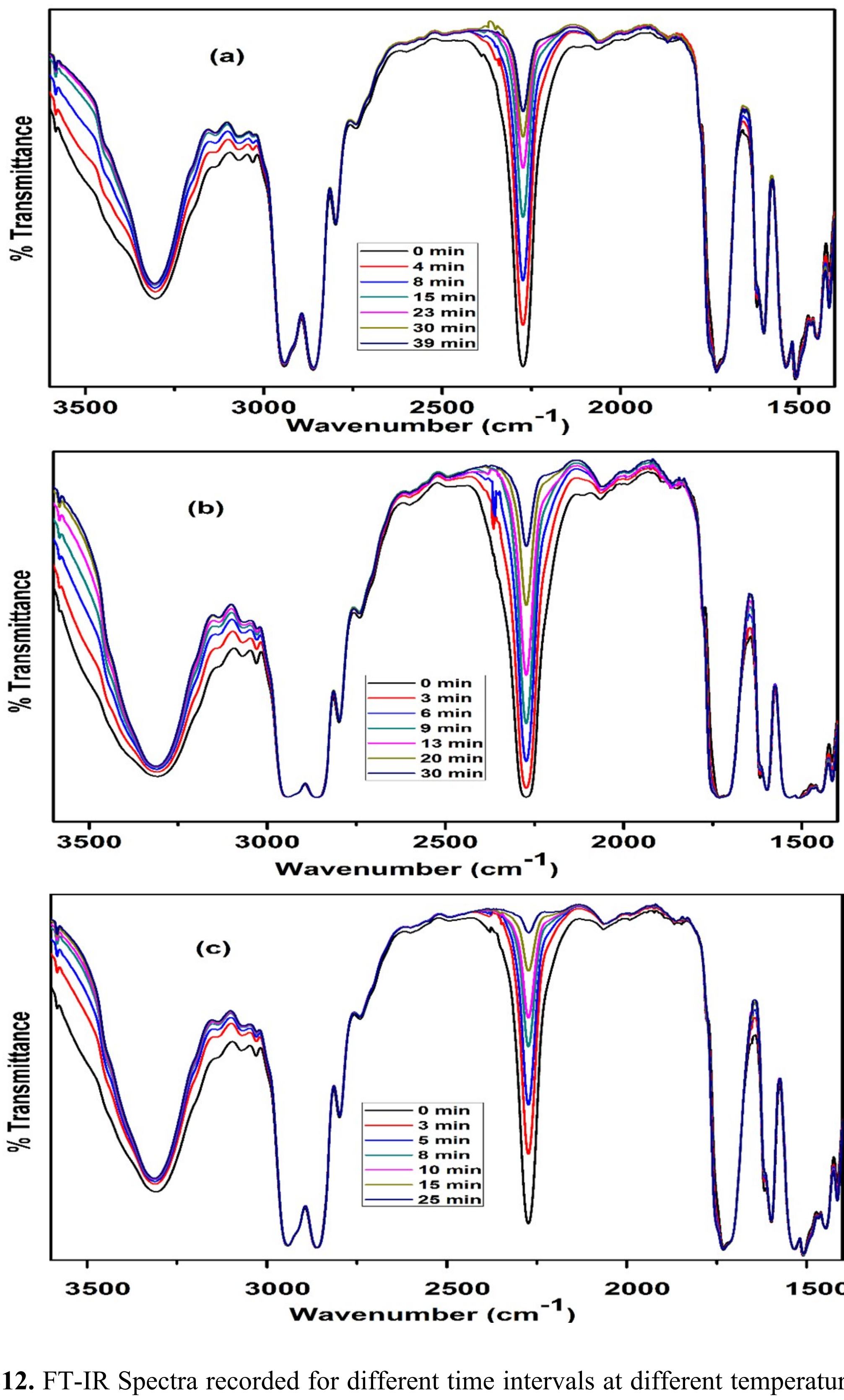

Figure S12. FT-IR Spectra recorded for different time intervals at different temperatures for the blocking reaction of polyisocyanate with p-methoxyphenol; (a) 40 ^{0}C (b) 50 ^{0}C and (c) 60 ^{0}C.

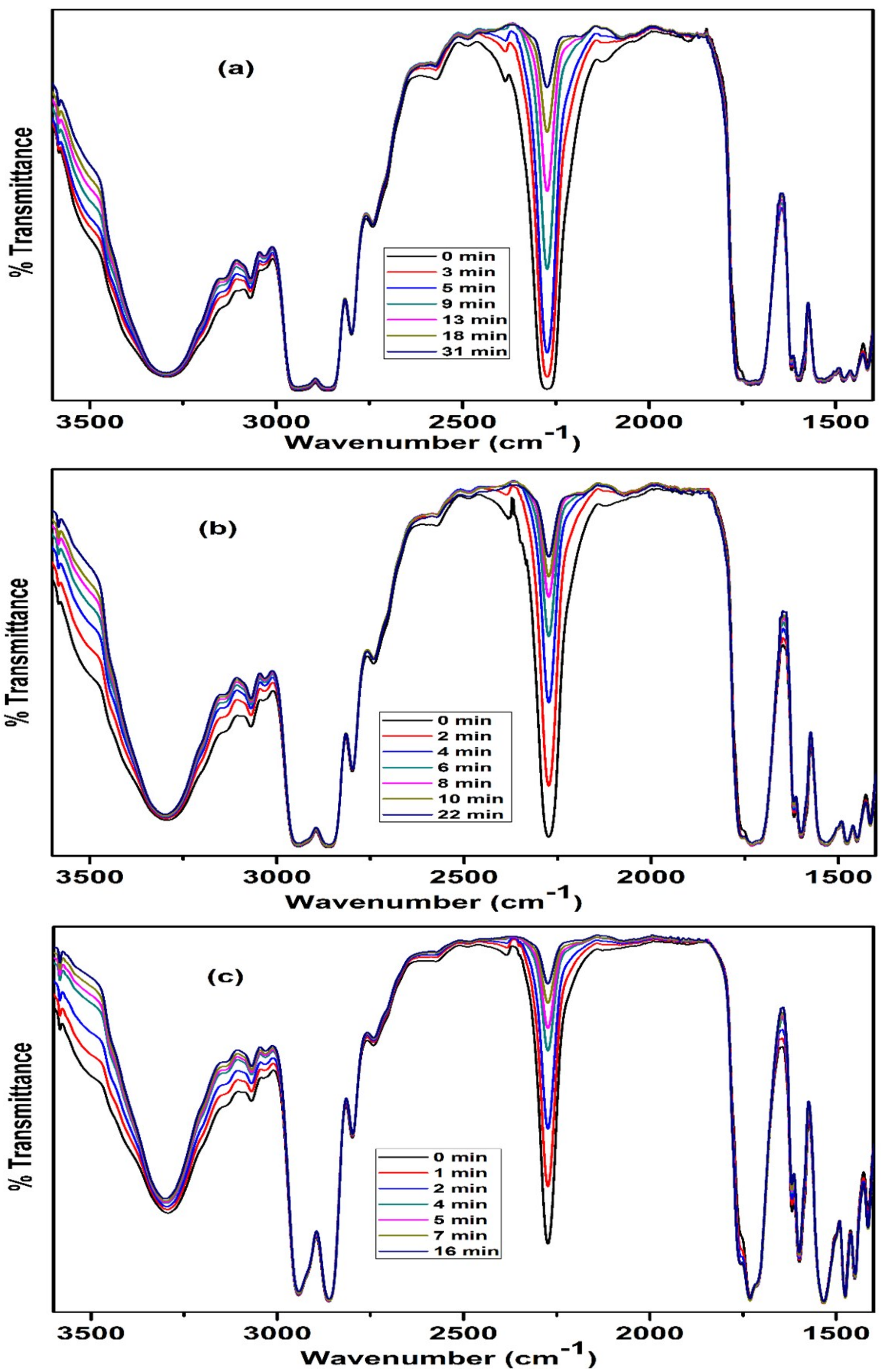

Figure S13. FT-IR Spectra recorded for different time intervals at different temperatures for the blocking reaction of polyisocyanate with o-chlorophenol; (a) 40 ^{0}C (b) 50 ^{0}C and (c) 60 ^{0}C.

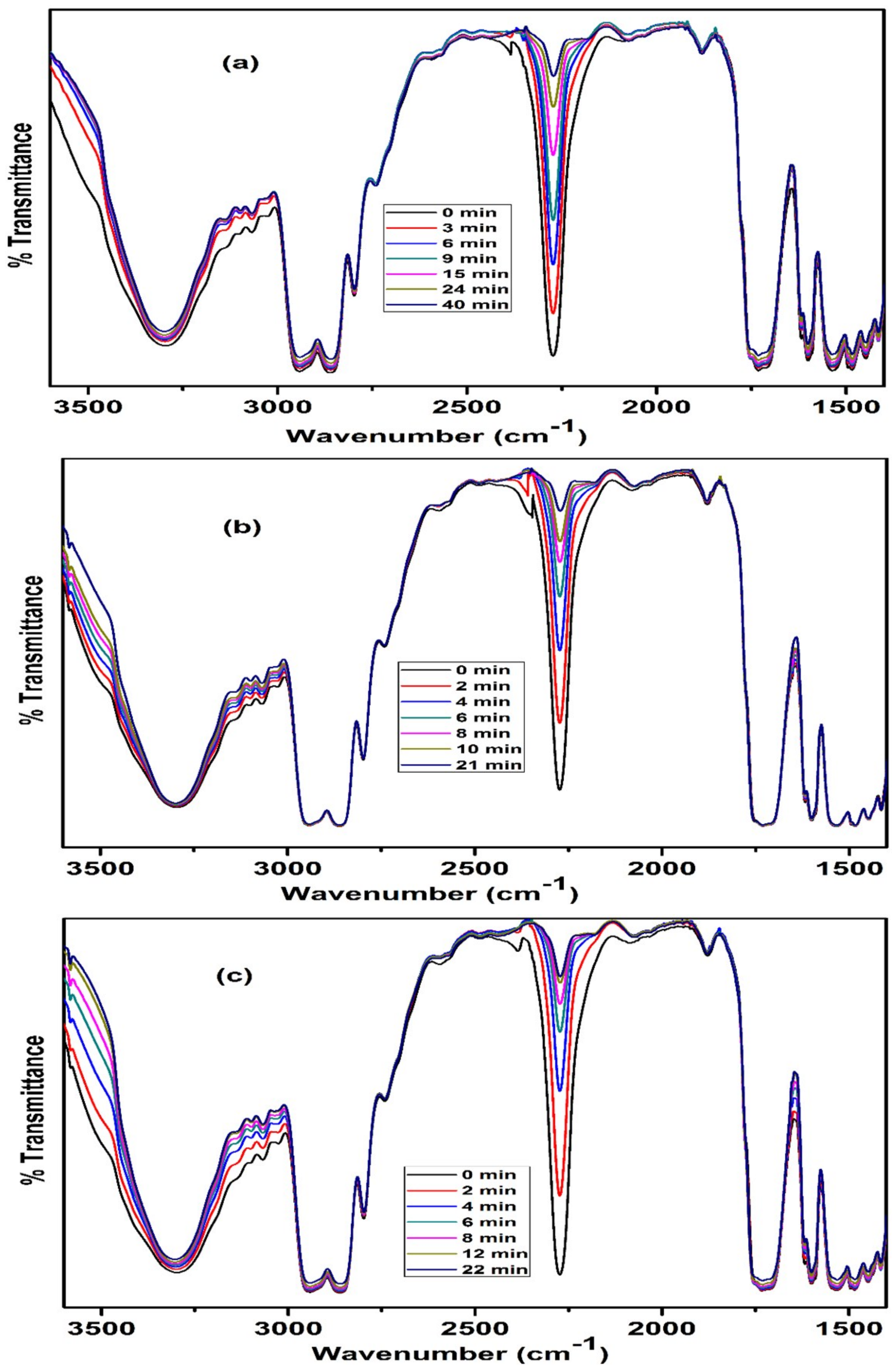

Figure S14. FT-IR Spectra recorded for different time intervals at different temperatures for the blocking reaction of polyisocyanate with p-chlorophenol; (a) 40 ^{0}C (b) 50 ^{0}C and (c) 60 ^{0}C.

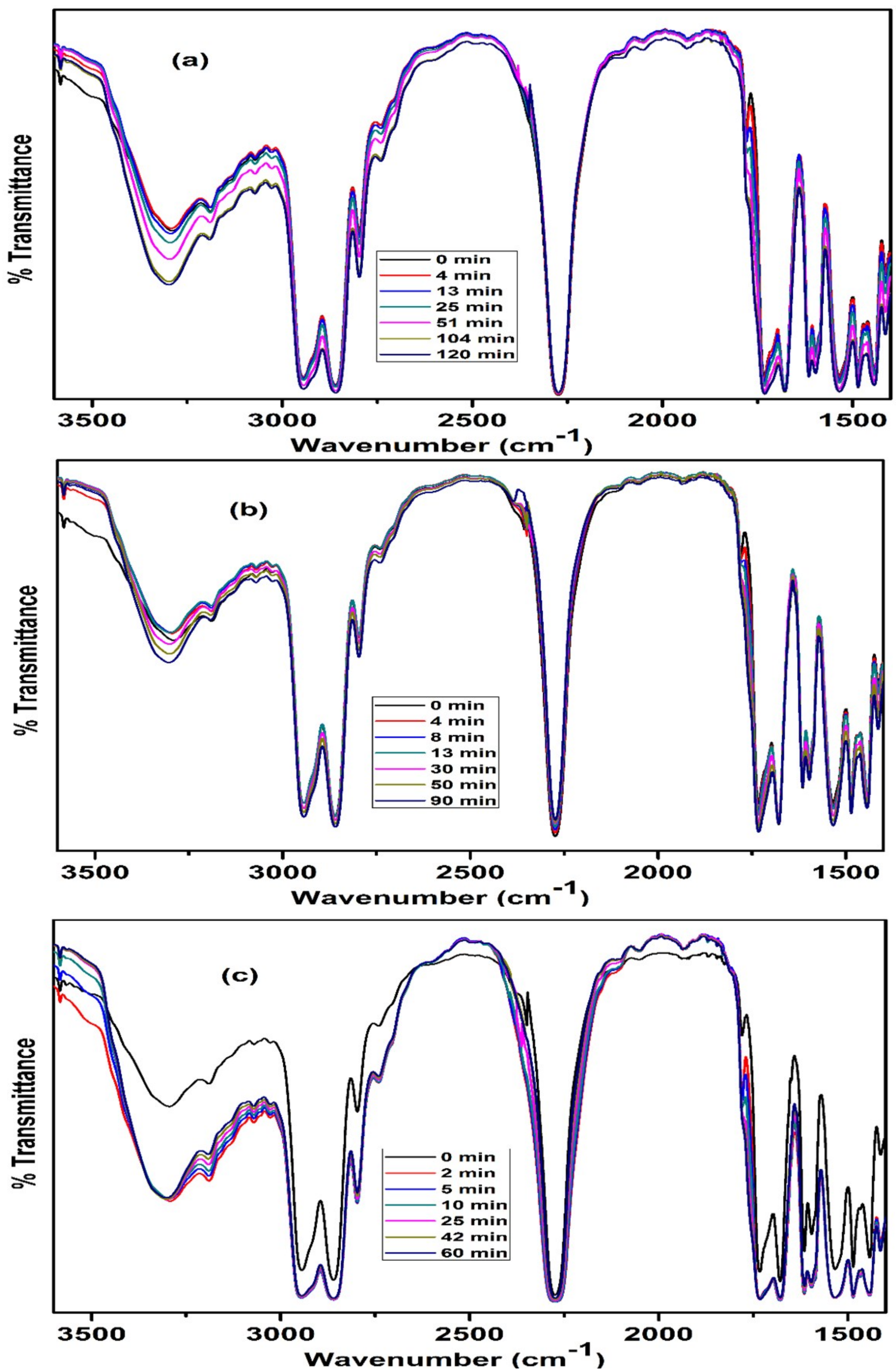

Figure S15. FT-IR Spectra recorded for different time intervals at different temperatures for the blocking reaction of polyisocyanate with o-esterphenol; (a) 40 ^{0}C (b) 50 ^{0}C and (c) 60 ^{0}C.

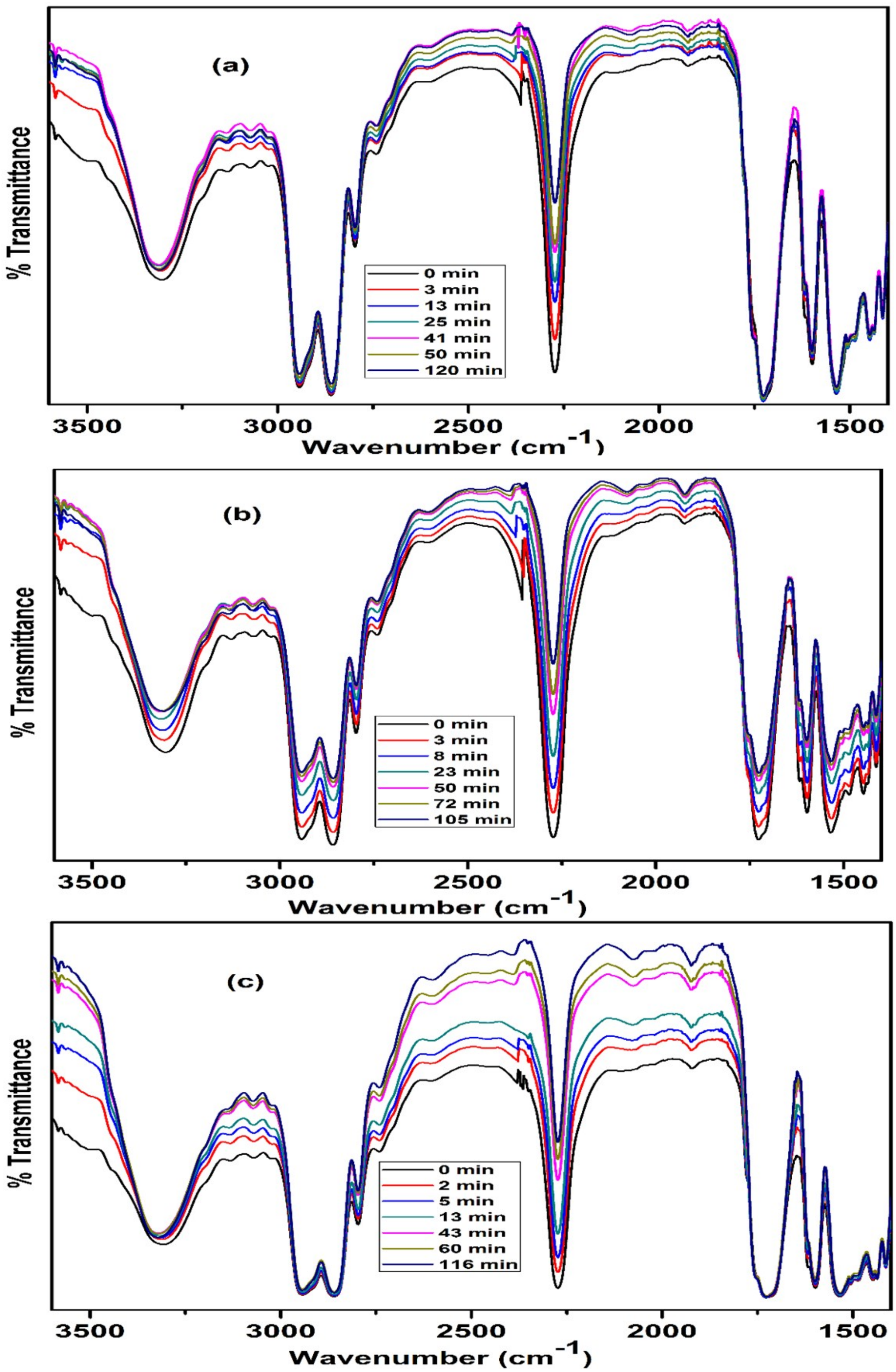

Figure S16. FT-IR Spectra recorded for different time intervals at different temperatures for the blocking reaction of polyisocyanate with p-esterphenol; (a) 40 ^{0}C (b) 50 ^{0}C and (c) 60 ^{0}C.

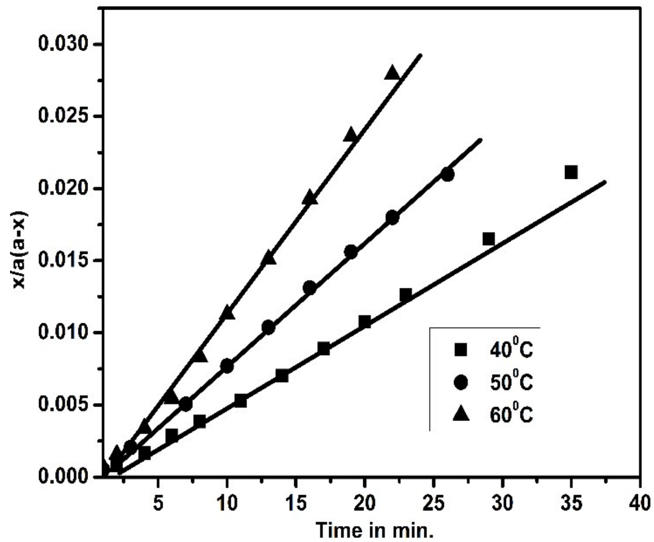

Figure S17. Amine-catalysed second-order kinetic plots of blocking reaction of polyisocyanate with o-cresol.

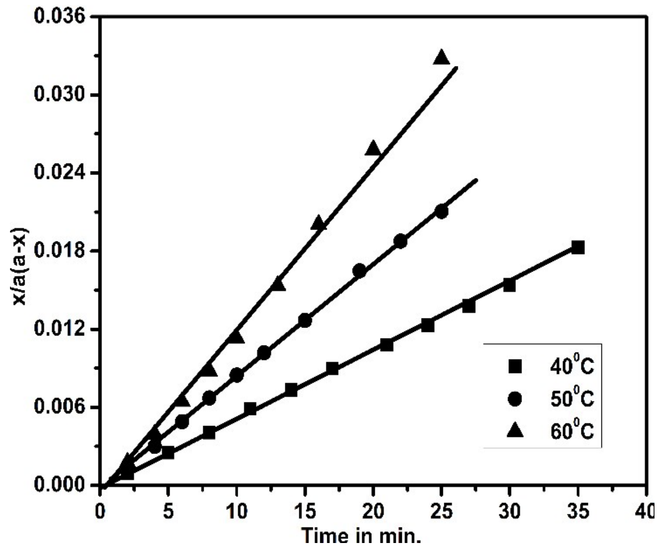

Figure S18. Amine-catalysed second-order kinetic plots of blocking reaction of polyisocyanate with p-cresol.

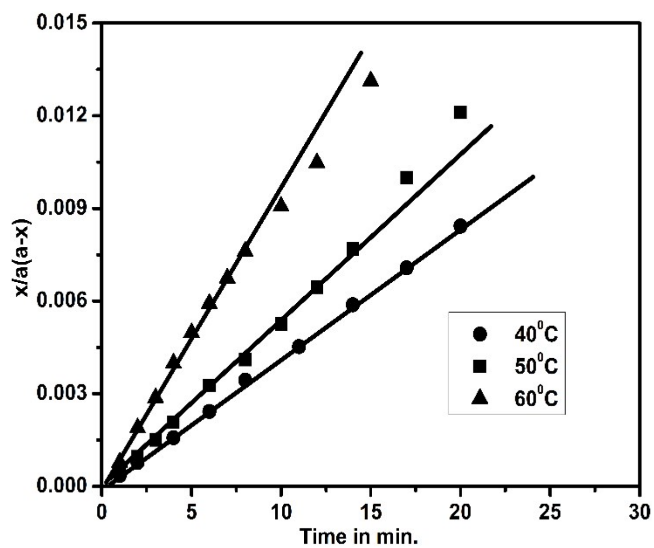

Figure S19. Amine-catalysed second-order kinetic plots of blocking reaction of polyisocyanate with o-methoxyphenol

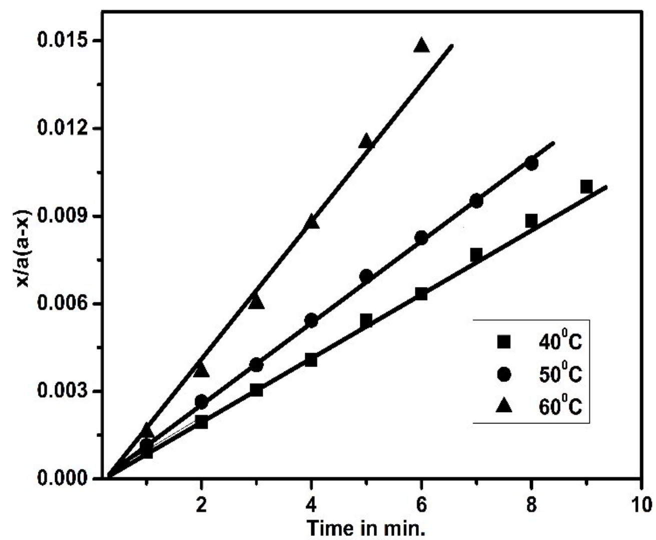

Figure S20. Amine-catalysed second-order kinetic plots of blocking reaction of polyisocyanate with p-methoxyphenol.

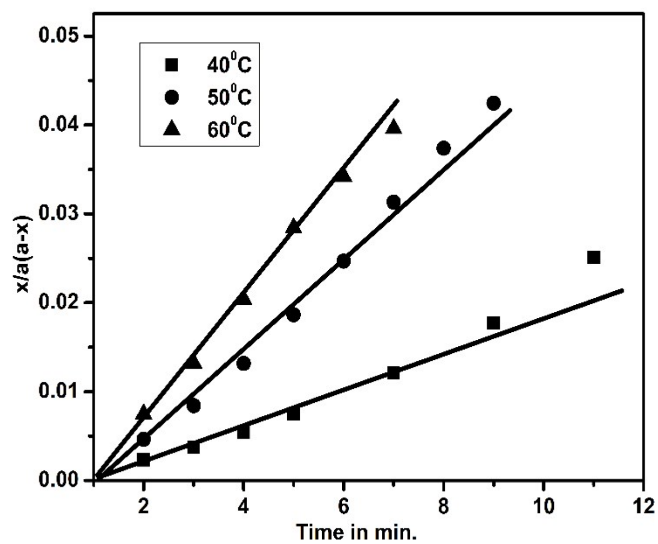

Figure S21. Amine-catalysed second-order kinetic plots of blocking reaction of polyisocyanate with o-chlorophenol.

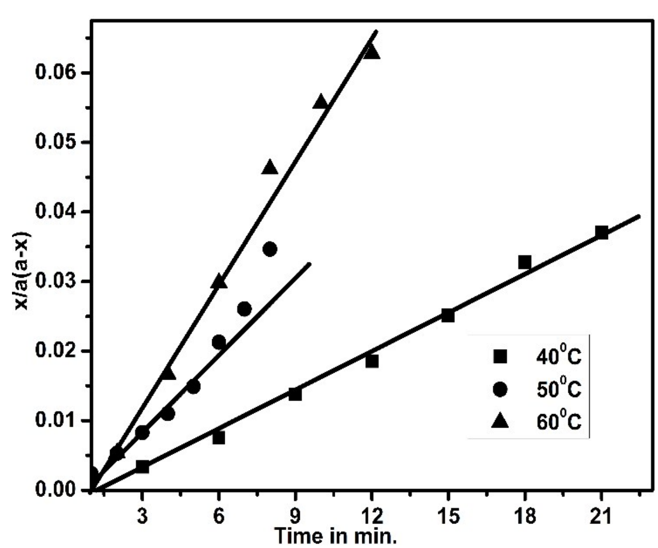

Figure S22. Amine-catalysed second-order kinetic plots of blocking reaction of polyisocyanate with p-chlorophenol.

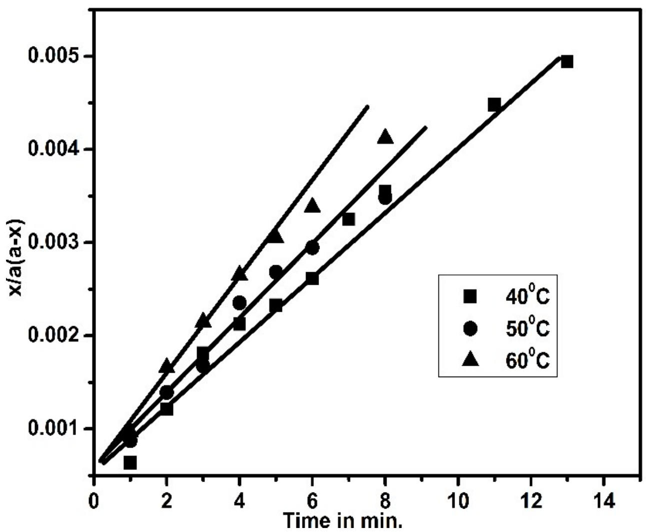

Figure S23. Amine-catalysed second-order kinetic plots of blocking reaction of polyisocyanate with o-esterphenol.

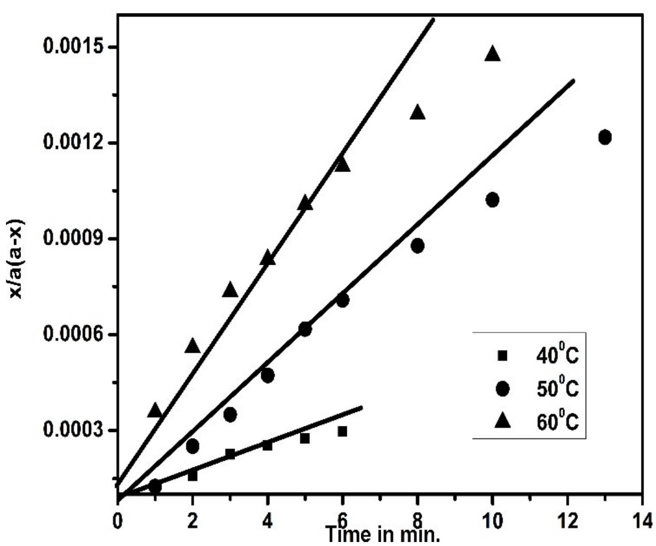

Figure S24. Amine-catalysed second-order kinetic plots of blocking reaction of polyisocyanate with p-esterphenol.

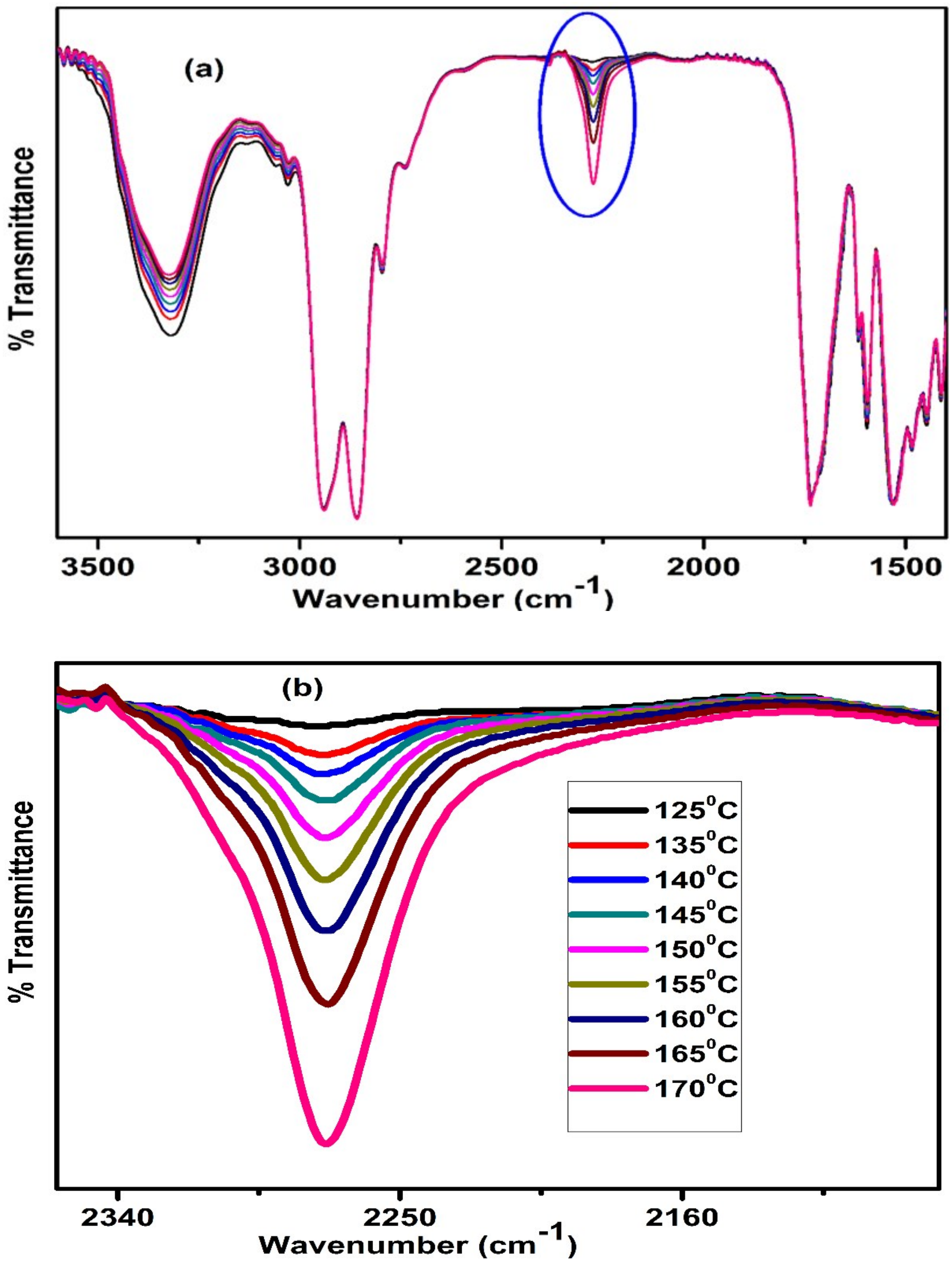

Figure S25. FT-IR spectra of o-cresol-blocked polyisocyanate recorded at (a) different temperatures. (b) Zoomed range of isocyanate absorption region.

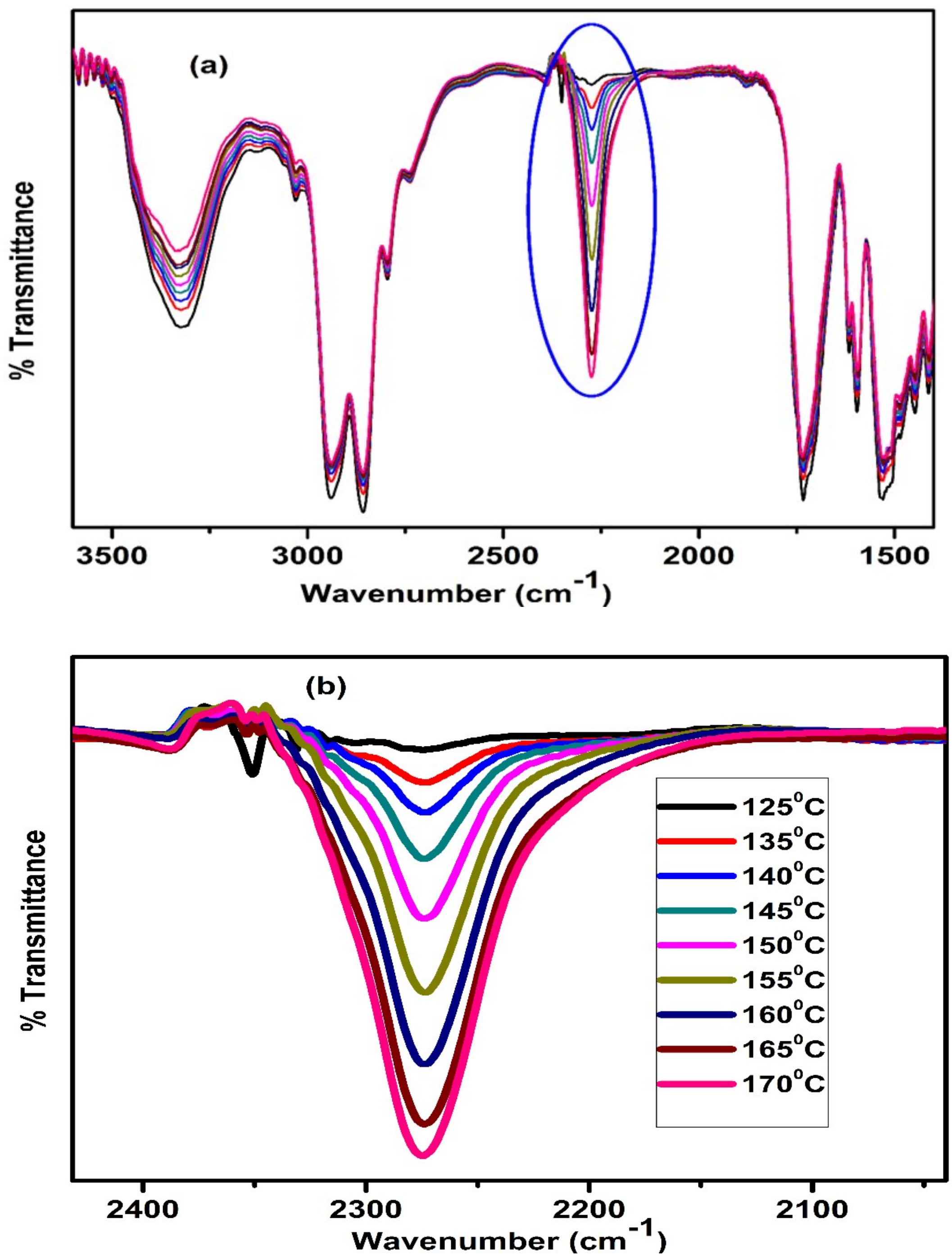

Figure S26. FT-IR spectra of p-cresol-blocked polyisocyanate recorded at (a) different temperatures. (b) Zoomed range of isocyanate absorption region.

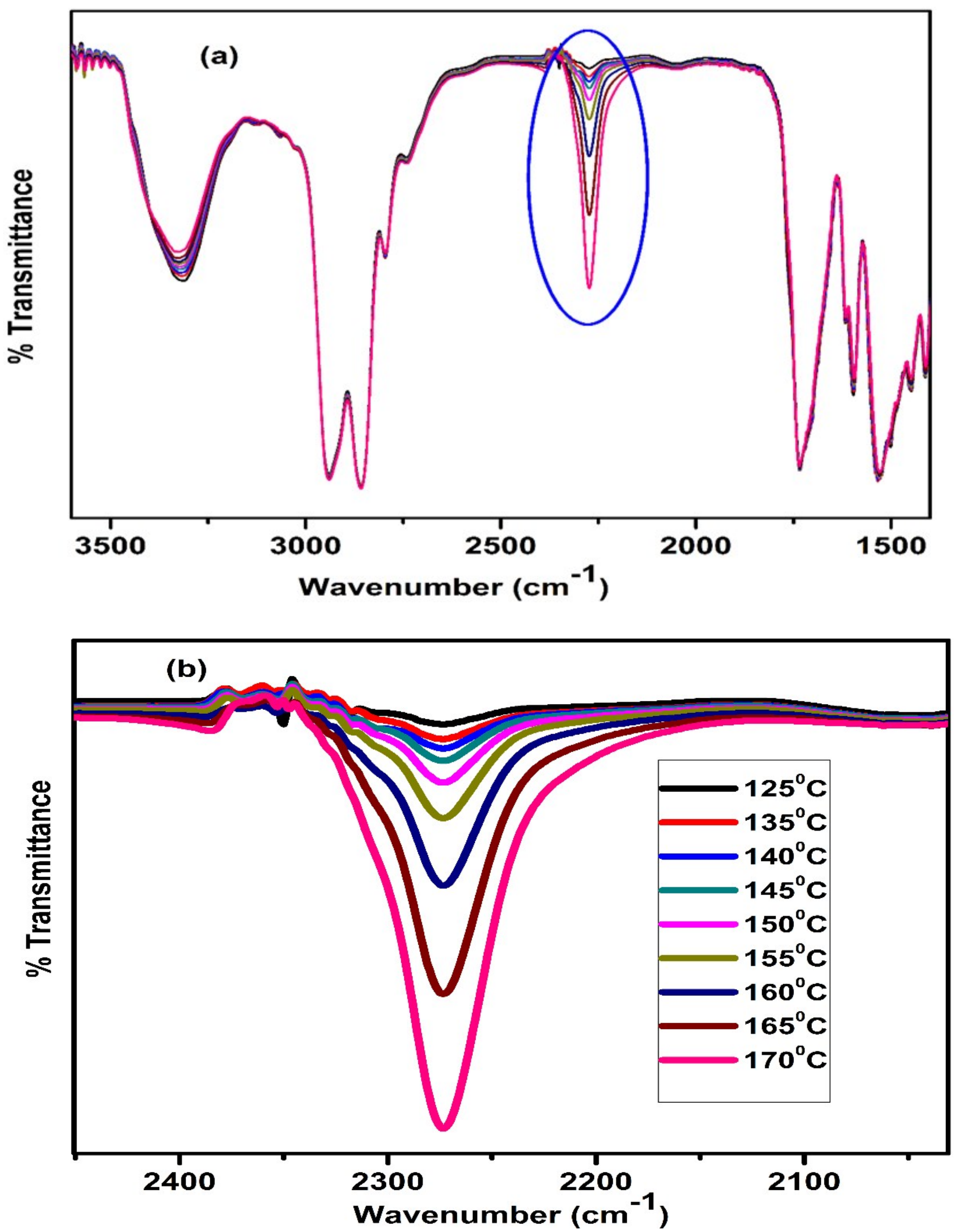

Figure S27. FT-IR spectra of o-methoxyphenol-blocked polyisocyanate recorded at (a) different temperatures. (b) Zoomed range of isocyanate absorption region.

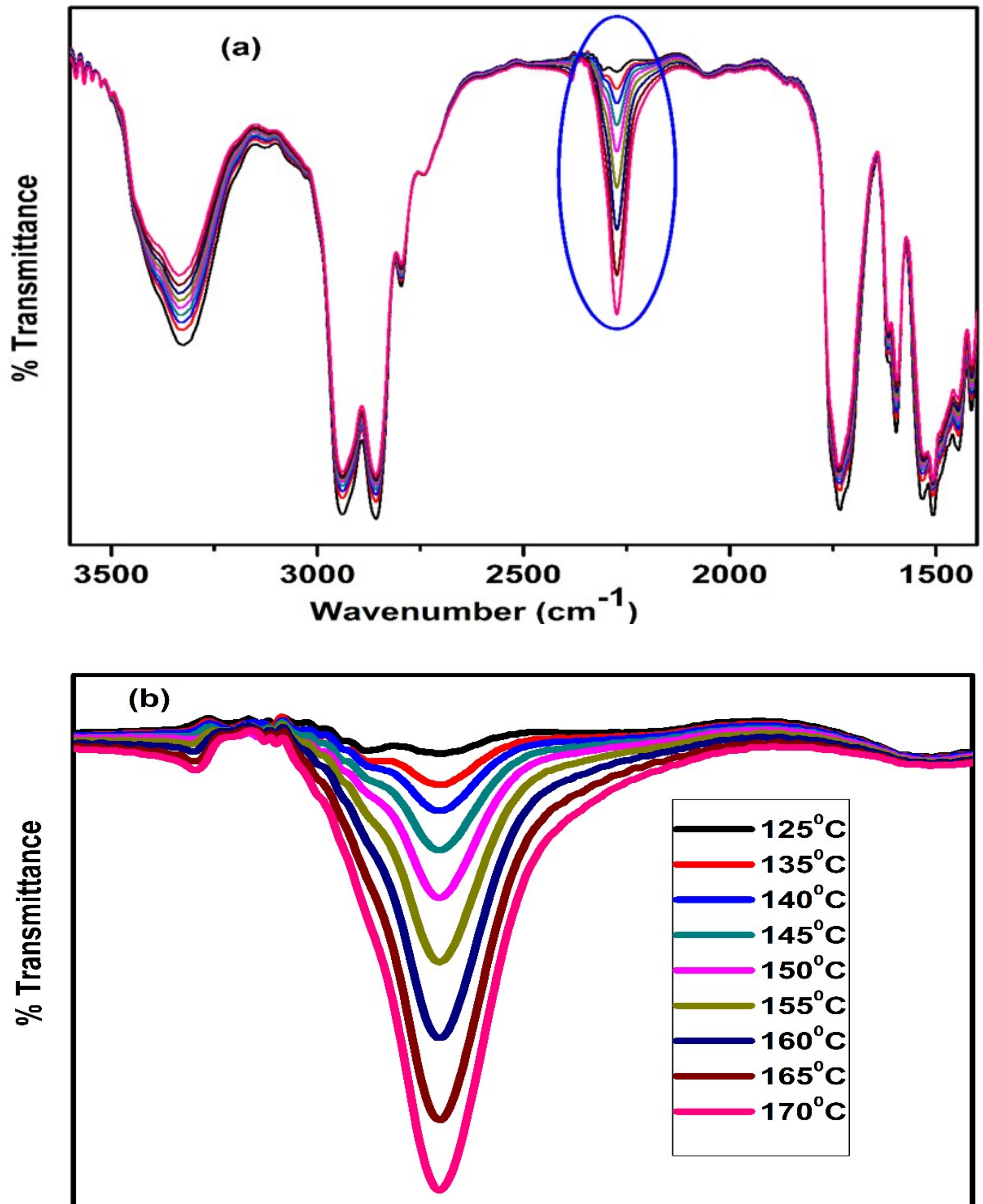

Figure S28. FT-IR spectra of p-methoxyphenol-blocked polyisocyanate recorded at (a) different temperatures. (b) Zoomed range of isocyanate absorption region.

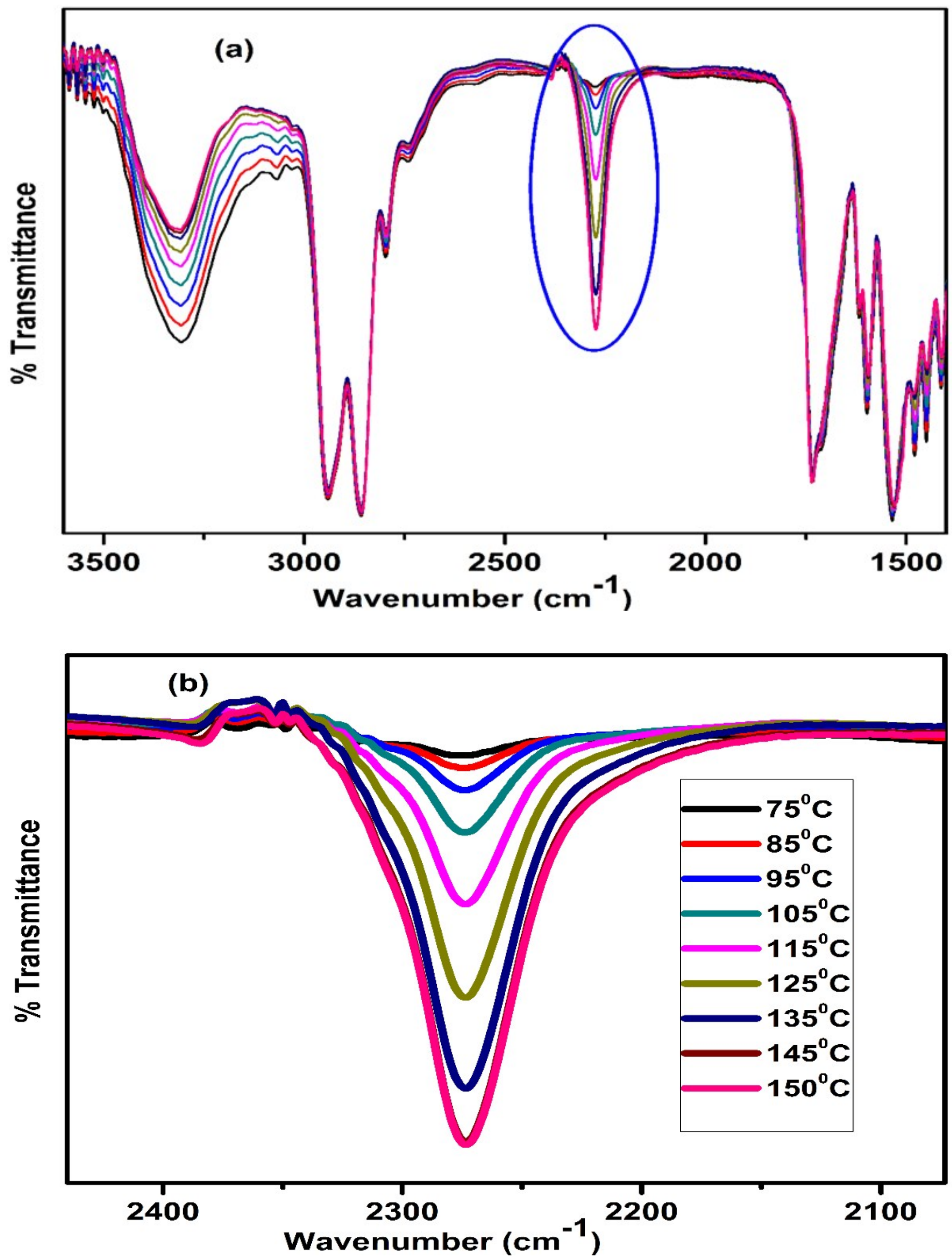

Figure S29. FT-IR spectra of o-chlorophenol-blocked polyisocyanate recorded at (a) different temperatures. (b) Zoomed range of isocyanate absorption region.

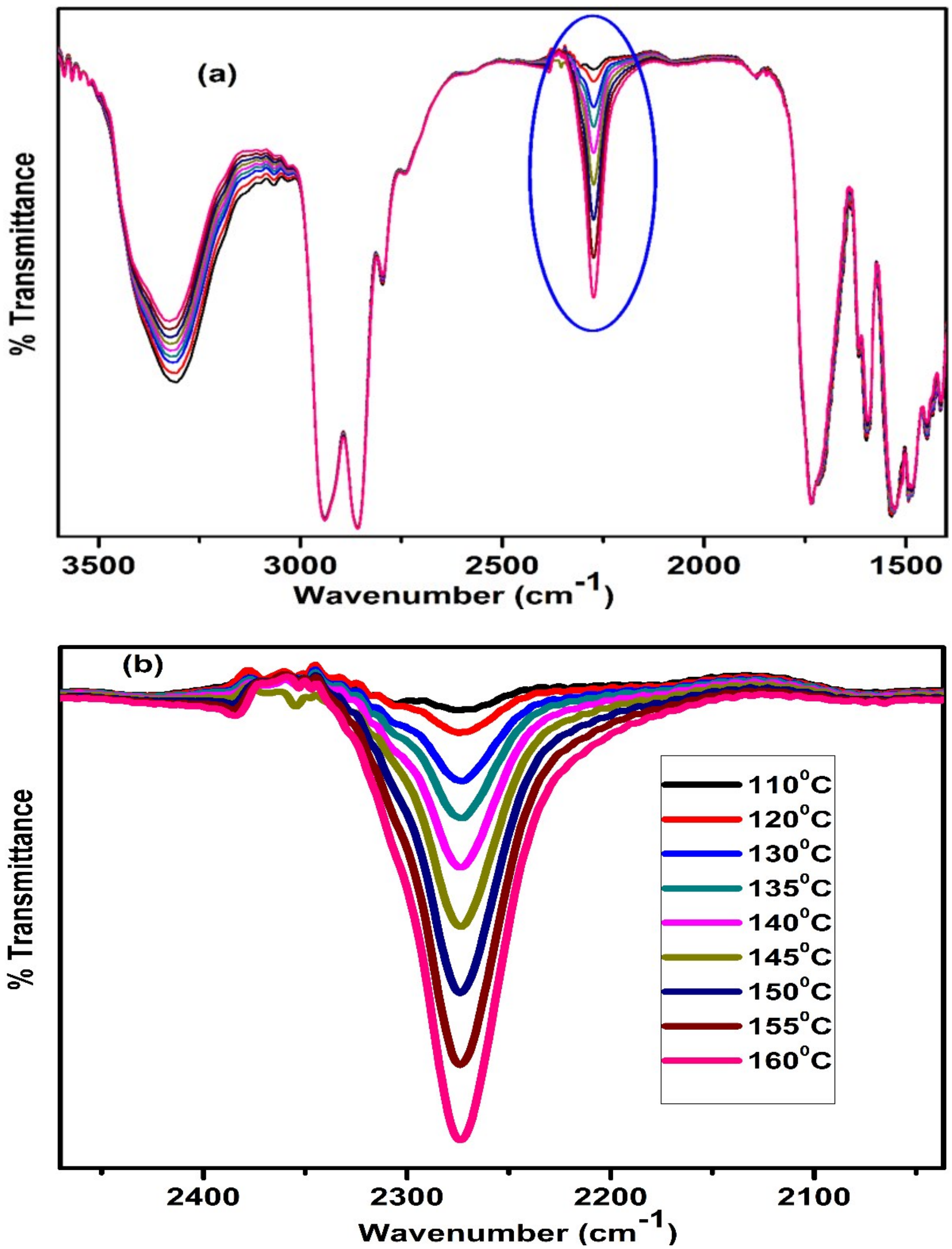

Figure S30. FT-IR spectra of p-chlorophenol-blocked polyisocyanate recorded at (a) different temperatures. (b) Zoomed range of isocyanate absorption region.

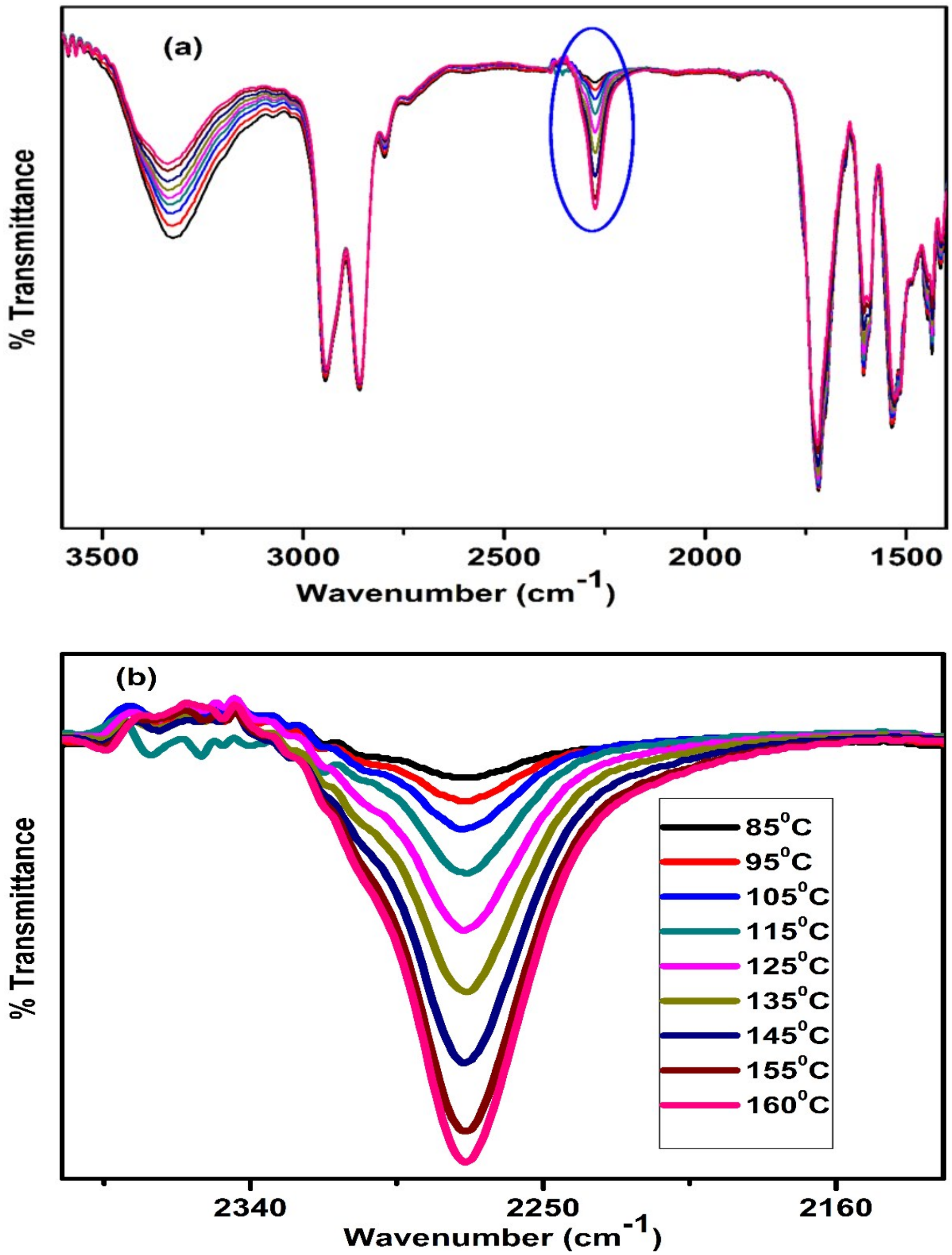

Figure S31. FT-IR spectra of p-esterphenol-blocked polyisocyanate recorded at (a) different temperatures. (b) Zoomed range of isocyanate absorption region.

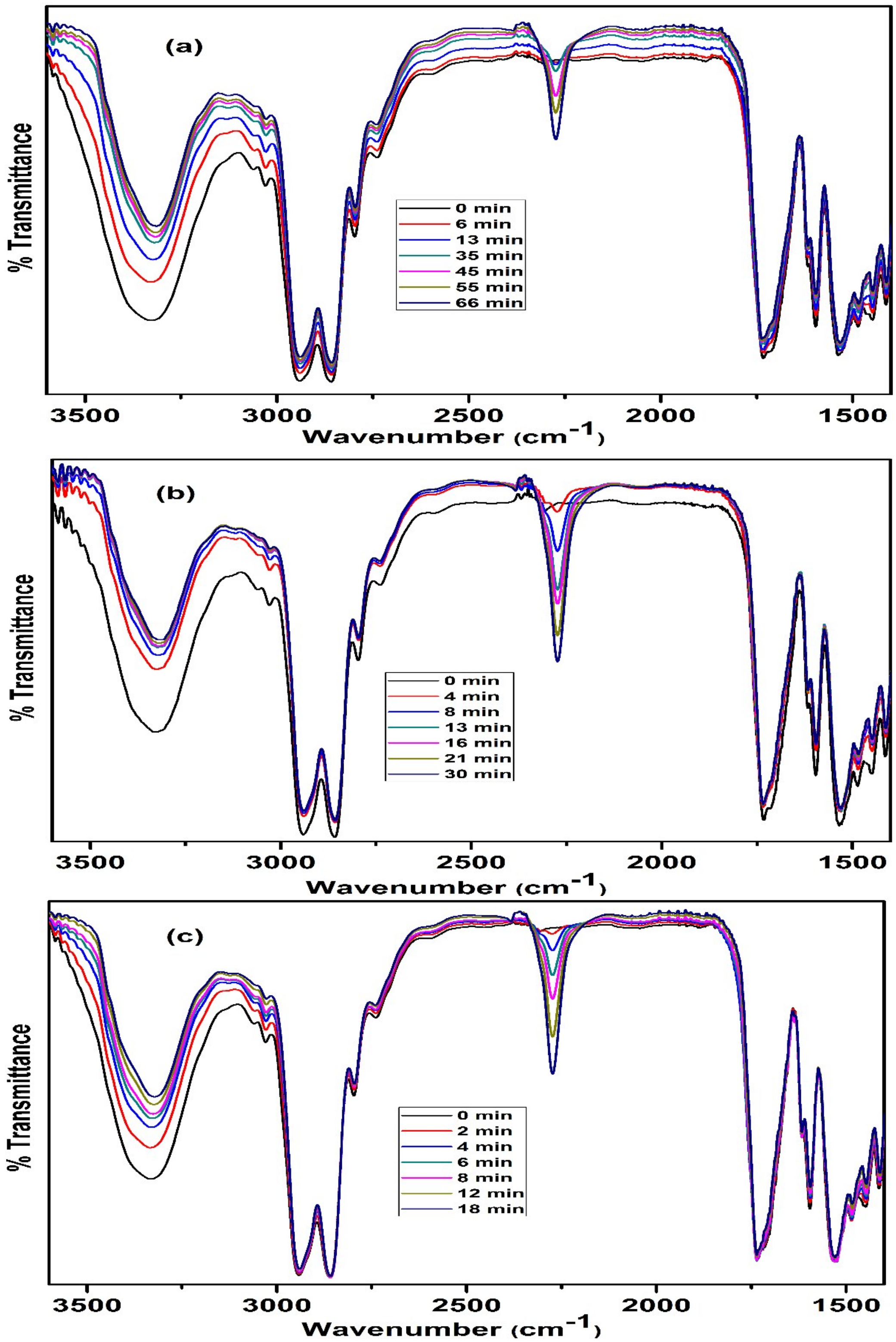

Figure S32. FT-IR Spectra recorded for different time intervals at different temperatures for the deblocking reaction of o-cresol-blocked polyisocyanate; (a) 120 ^{0} (b) 130 ^{0}C and (c) 140 ^{0}C.

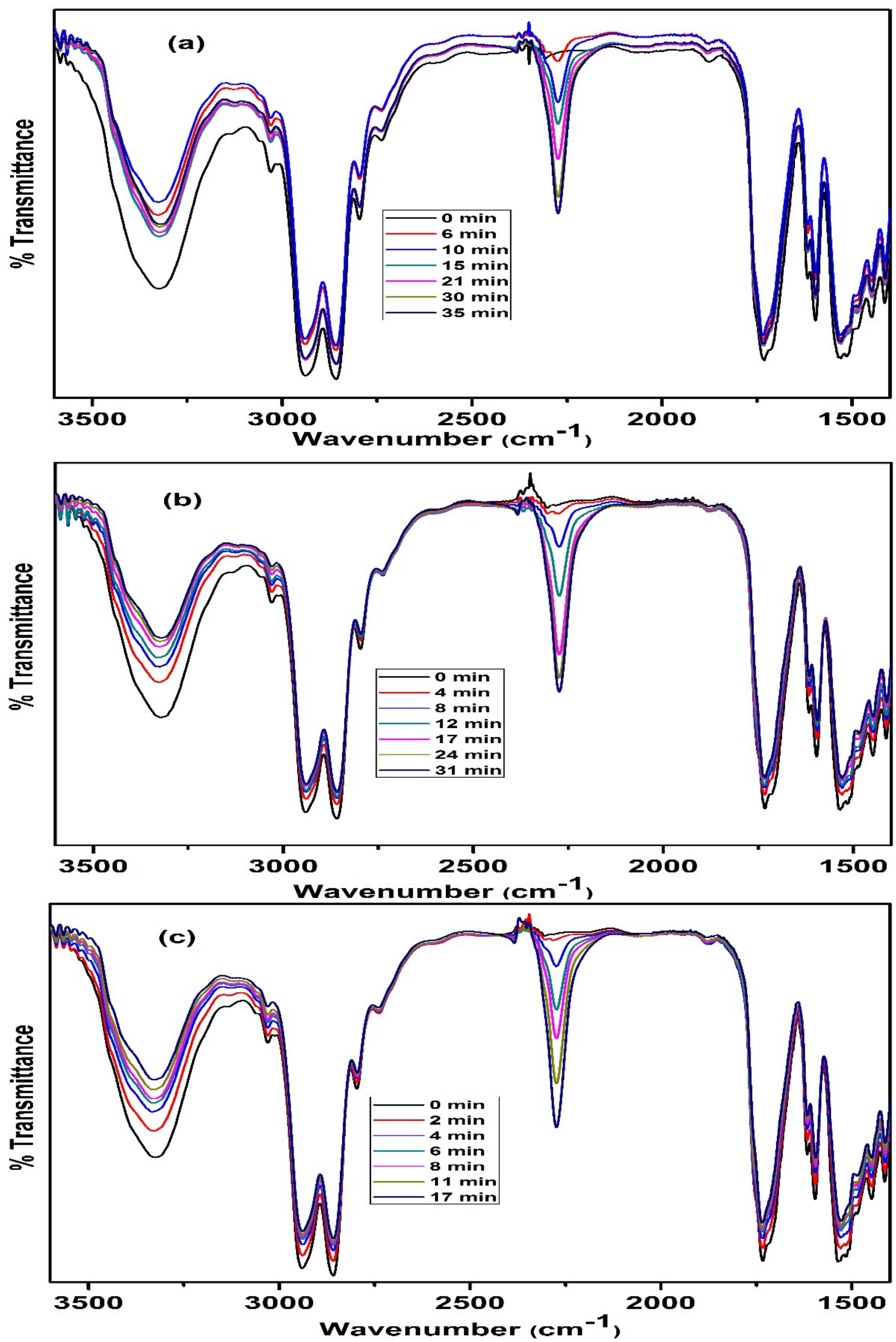

Figure S33. FT-IR Spectra recorded for different time intervals at different temperatures for the deblocking reaction of p-cresol-blocked polyisocyanate; (a) 120 ^{0}C (b) 130 ^{0}C and (c) 140 ^{0}C.

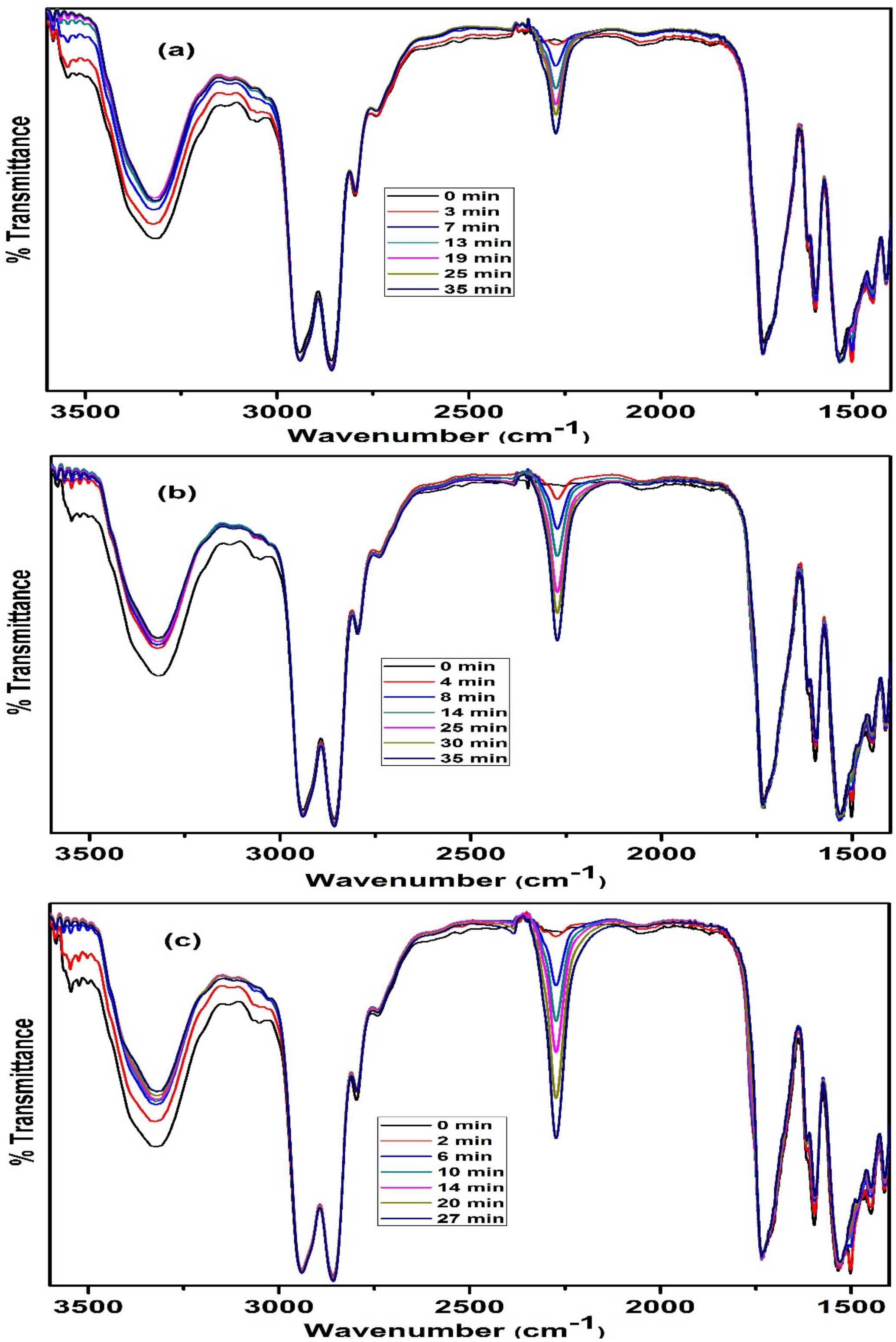

Figure S34. FT-IR Spectra recorded for different time intervals at different temperatures for the deblocking reaction of o-methoxyphenol-blocked polyisocyanate; (a) 120 ^{0}C (b) 130 ^{0}C and (c) 140 ^{0}C.

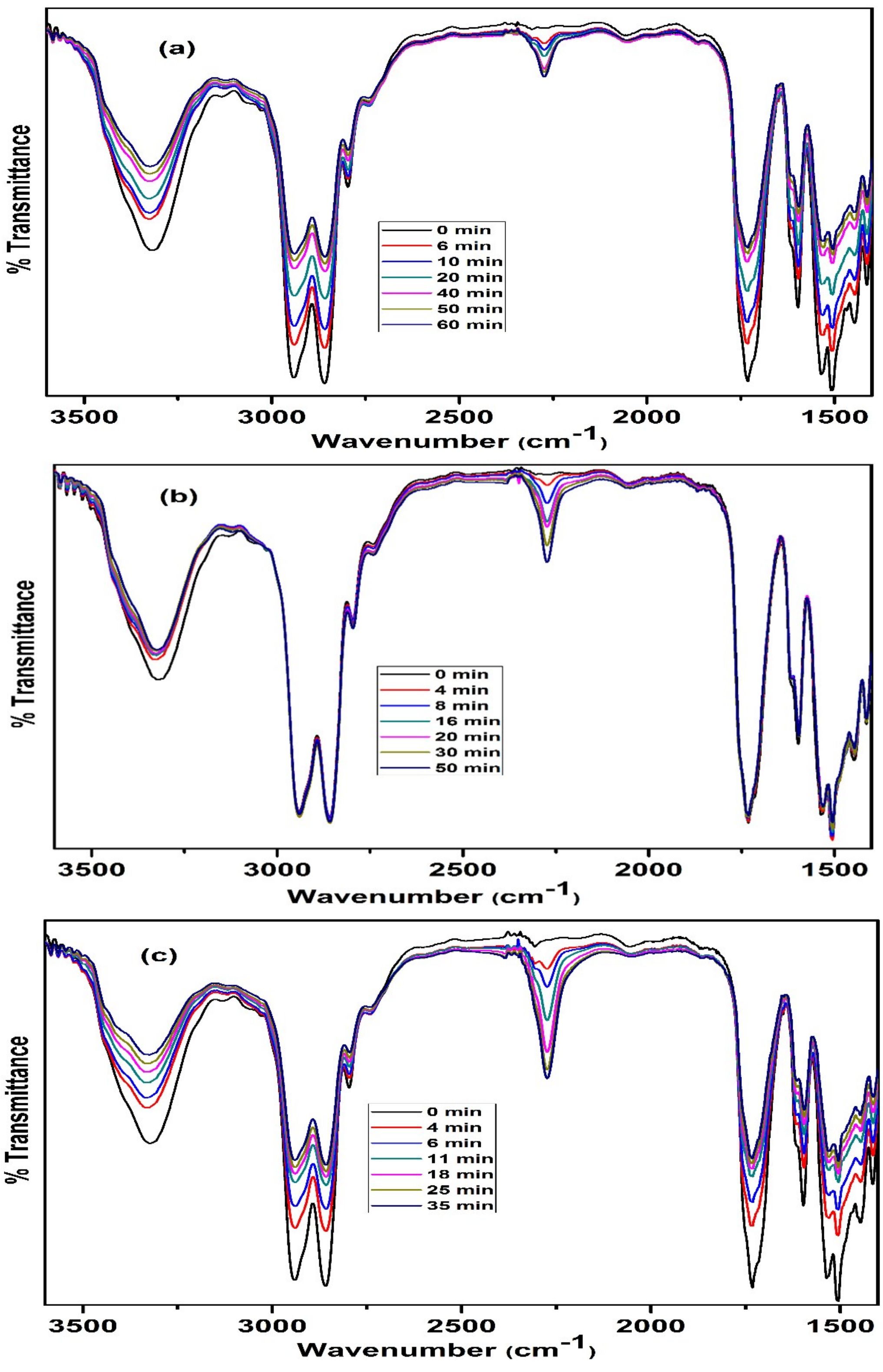

Figure S35. FT-IR Spectra recorded for different time intervals at different temperatures for the deblocking reaction of p-methoxyphenol-blocked polyisocyanate; (a) 120 ^{0}C (b) 130 ^{0}C and (c) 140 ^{0}C.

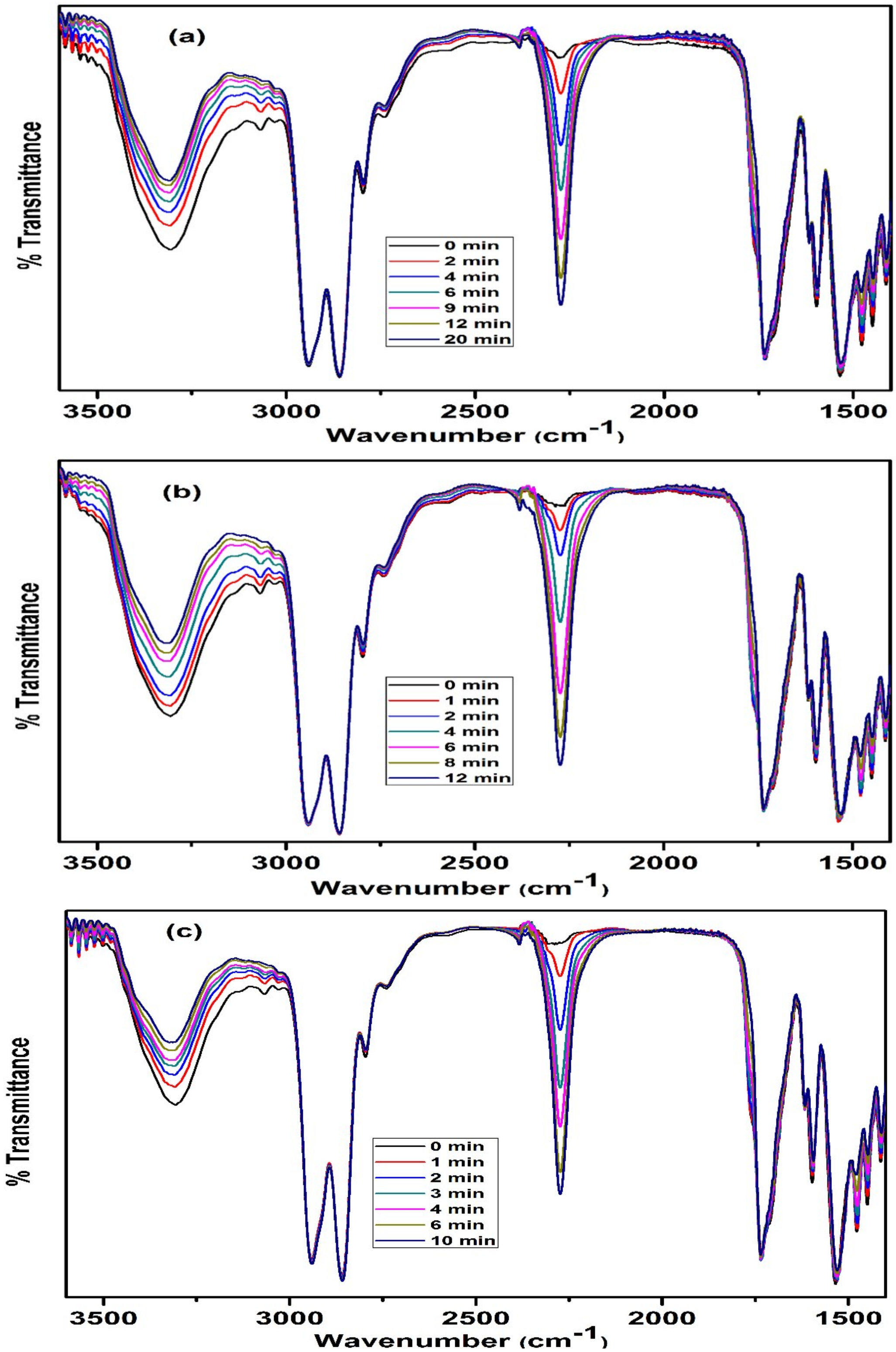

Figure S36. FT-IR Spectra recorded for different time intervals at different temperatures for the deblocking reaction of o-chlorophenol-blocked polyisocyanate; (a) 120 ^{0}C (b) 130 ^{0}C and (c) 140 ^{0}C.

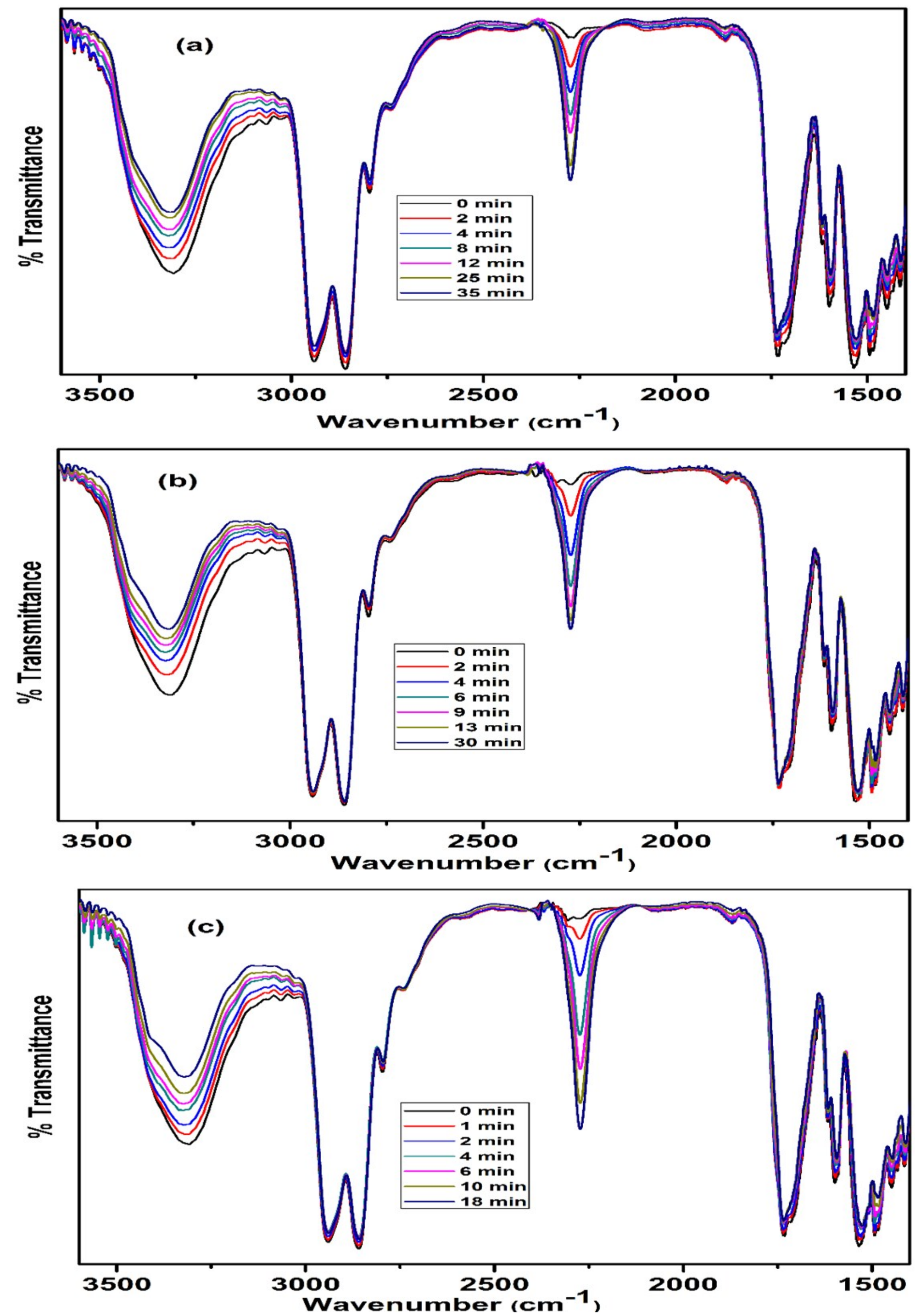

Figure S37. FT-IR Spectra recorded for different time intervals at different temperatures for the deblocking reaction of p-chlorophenol-blocked polyisocyanate; (a) 120 ^{0}C (b) 130 ^{0}C and (c) 140 ^{0}C.

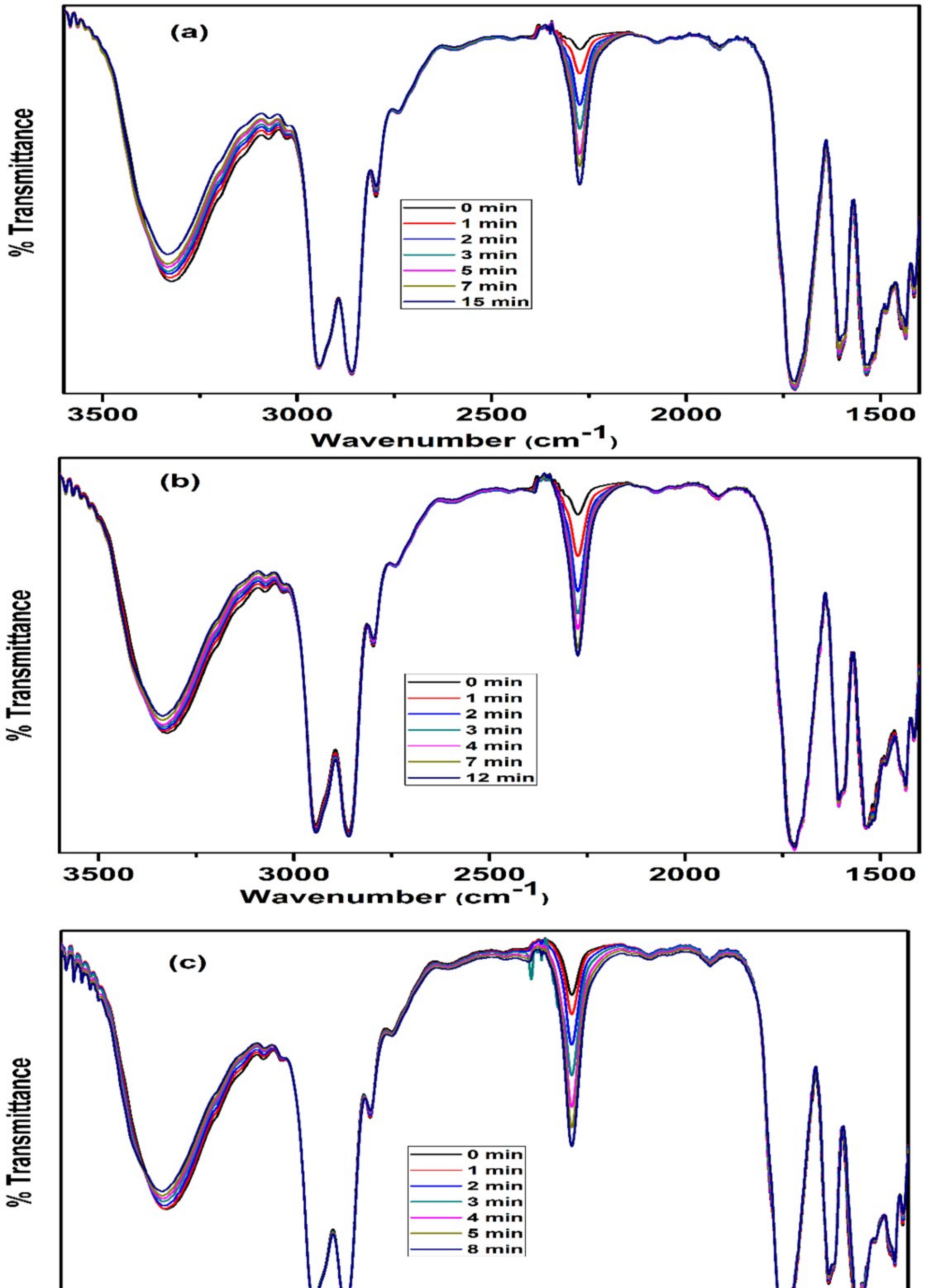

Figure S38. FT-IR Spectra recorded for different time intervals at different temperatures for the deblocking reaction of p-esterphenol-blocked polyisocyanate; (a) 120 ^{0}C (b) 130 ^{0}C and (c) 140 ^{0}C.

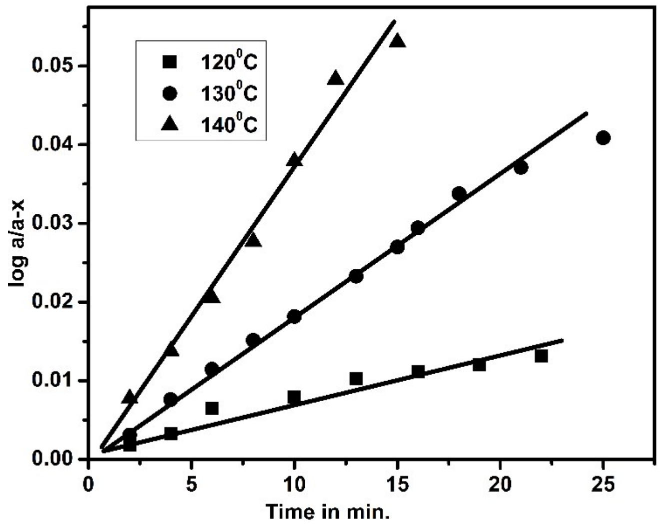

Figure S39. Amine-catalysed first-order kinetic plots of deblocking reaction of o-cresol blocked polyisocyanate.

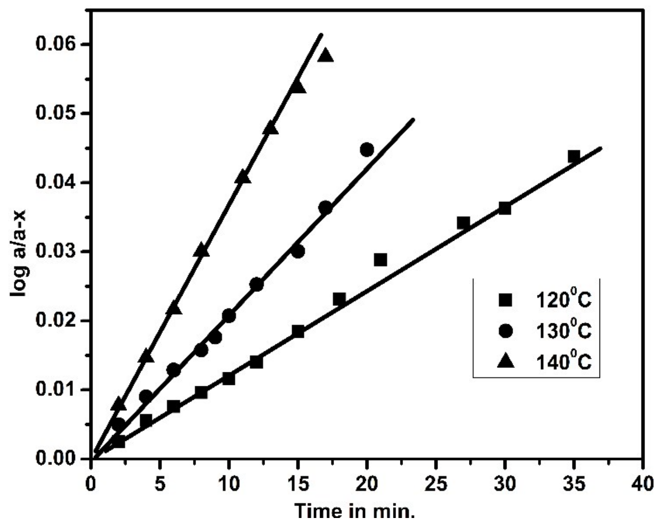

Figure S40. Amine-catalysed first-order kinetic plots of deblocking reaction of p-cresol blocked polyisocyanate.

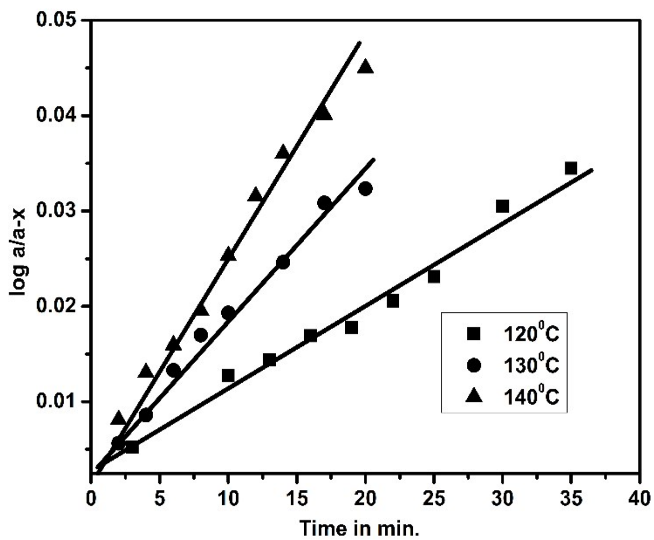

Figure S41. Amine-catalysed first-order kinetic plots of deblocking reaction of o-methoxyphenol blocked polyisocyanate.

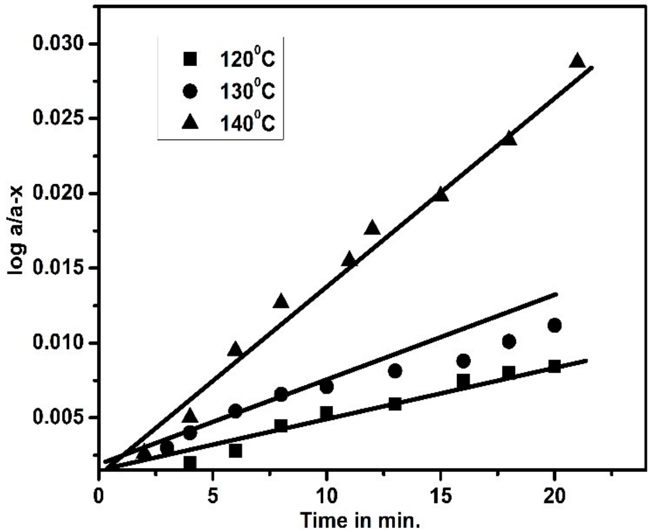

Figure S42. Amine-catalysed first-order kinetic plots of deblocking reaction of p-methoxyphenol blocked polyisocyanate.

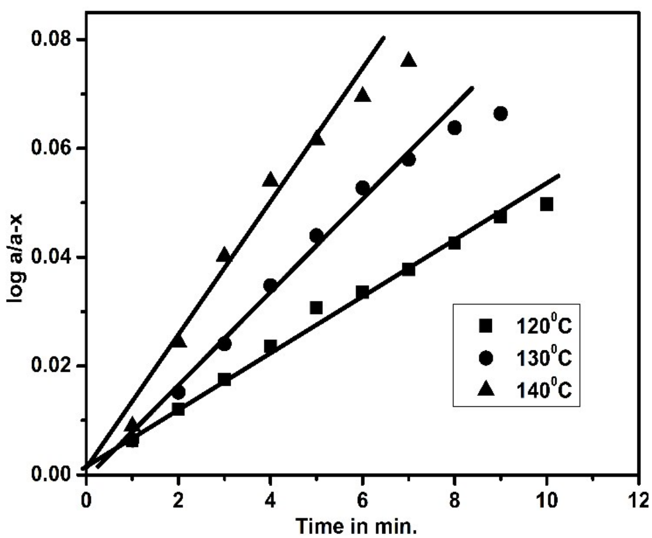

Figure S43. Amine-catalysed first-order kinetic plots of deblocking reaction of o-chlorophenol blocked polyisocyanate.

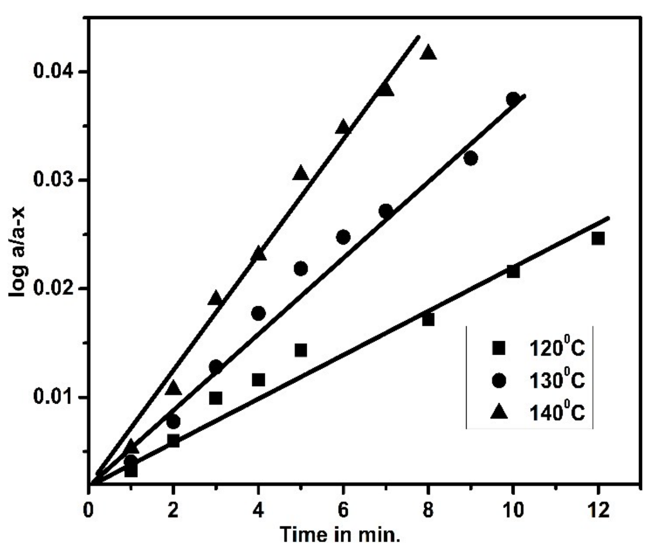

Figure S44. Amine-catalysed first-order kinetic plots of deblocking reaction of p-chlorophenol blocked polyisocyanate.

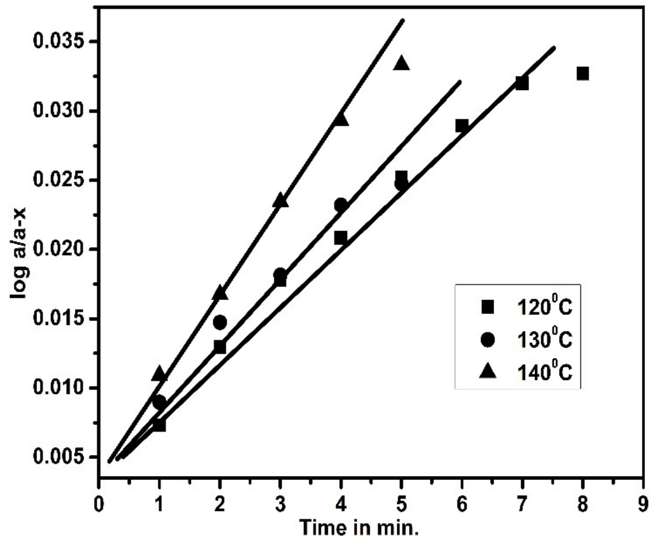

Figure S45. Amine-catalysed first-order kinetic plots of deblocking reaction of p-esterphenol blocked polyisocyanate.

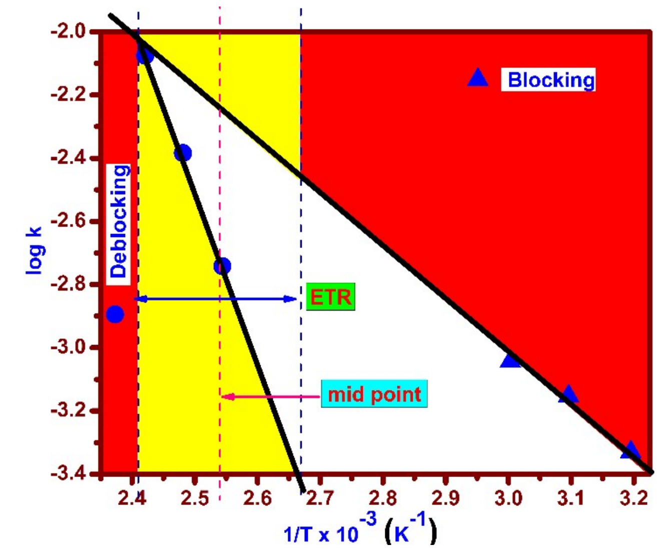

Figure S46. Arrhenius plots of forward and reverse reactions of o-cresol-blocked polyisocyante showing equilibrium temperature range (ETR) and probable equilibrium temperature.

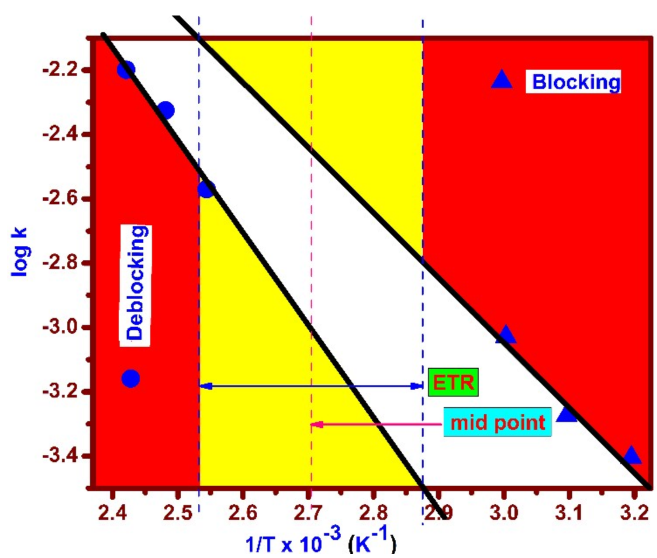

Figure S47. Arrhenius plots of forward and reverse reactions of p-cresol-blocked polyisocyante showing equilibrium temperature range (ETR) and probable equilibrium temperature.

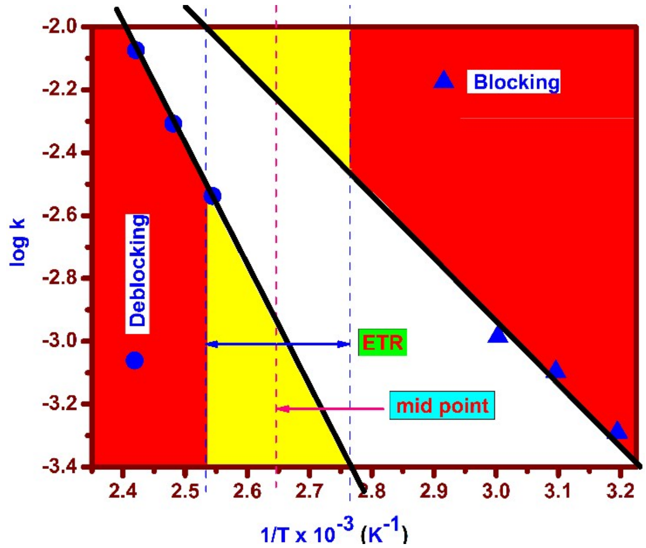

Figure S48. Arrhenius plots of forward and reverse reactions of o-OMe-phenol-blocked polyisocyante showing equilibrium temperature range (ETR) and probable equilibrium temperature.

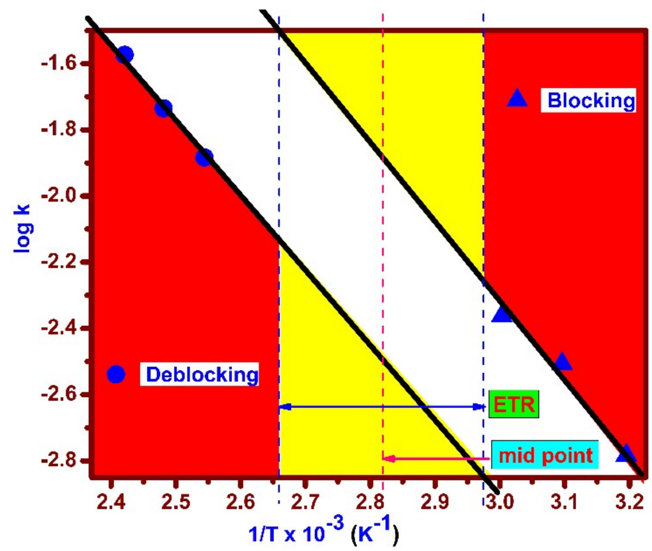

Figure S49. Arrhenius plots of forward and reverse reactions of o-Cl-phenol-blocked polyisocyante showing equilibrium temperature range (ETR) and probable equilibrium temperature.

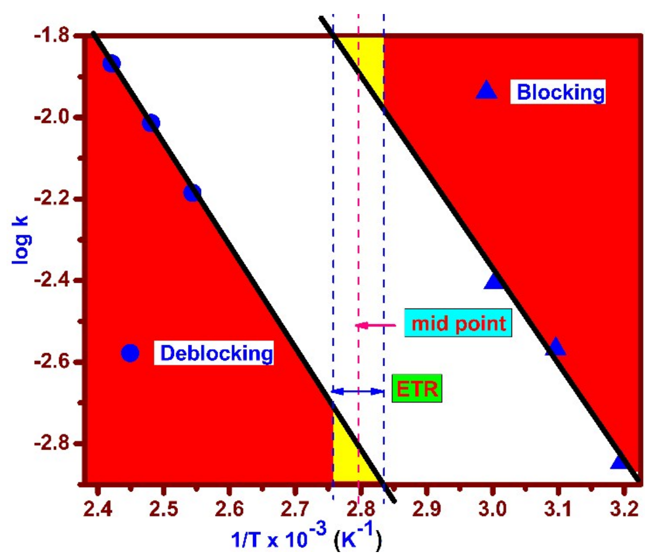

Figure S50. Arrhenius plots of forward and reverse reactions of p-Cl-phenol-blocked polyisocyante showing equilibrium temperature range (ETR) and probable equilibrium temperature.